2012

Characterization of the expression of the intercellular adhesin locus in Staphylococcus aureus

Jamie Brooks
Virginia Commonwealth University

CHARACTERIZATION OF THE EXPRESSION OF THE INTERCELLULAR ADHESIN LOCUS IN *STAPHYLOCOCCUS AUREUS*

A dissertation submitted in partial fulfillment of the requirements for the degree of Doctor of Philosophy at Virginia Commonwealth University.

by

JAMIE L. BROOKS
B.S., Lynchburg College 2006

Director: Kimberly K. Jefferson, Ph.D.
Associate Professor, Department of Microbiology and Immunology
Virginia Commonwealth University
Richmond, Virginia

Virginia Commonwealth University
Richmond, Virginia
December 2012

Acknowledgements

I would first like to express my heartfelt gratitude to my mentor Dr. Kimberly Jefferson. Her patient guidance and support in academic, scientific, and personal matters has enabled me to persevere and successfully complete my tenure as a graduate student with a project to be proud of. My development as an independent scientist would not have been possible without her mentorship.

I would also like to thank the members of my graduate advisory committee: Dr. Gordon Archer, Dr. Todd Kitten, Dr. Shirley Taylor, and Dr. Brad Windle. Their knowledge, advice, guidance, and constant questions during seminars and committee meetings have been invaluable. I would also like to think Dr. Gail Christie for her assistance working through research problems, and for allowing me such generous access to her laboratory resources and equipment.

Finally, I would like to sincerely thank all of my lab-mates, past and present: Dr. Karl Thompson, Dr. Nicole Mackey-Lawrence, Dr. Jennifer Patterson, Dr. Nabil Abraham, Dr. Michael Harwich, Dr. Nuno Cerca, Melissa Ray, and Melissa Prestosa. I will always appreciate their patience through countless meetings and practice presentations, as well as all of the input and feedback they've provided. A last very special note of my thanks is extended to Kristen Lane in Dr. Christie's lab. Her constant advice, humor, and friendship played a vital role in the successful completion of my doctoral training.

Dedication

I would like to dedicate this work to my husband and our daughters who have patiently encouraged and supported me in all that I have chosen to pursue. I would also like to dedicate this work to my mother, for her complete dedication to helping me achieve the best future possible through a lifetime of thoughtful guidance and complete support. My successes have been made possible by the involvement of my loved ones.

Table of Contents

List of Figures

List of Tables

Page

List of Abbreviations

°C ..... degrees centigrade
µg ..... microgram
µl ..... microliter
A ..... adenosine
Amp ..... ampicillin
Amp^r ..... ampicillin resistance
AMPs ..... antimicrobial peptides
APS ..... ammonium persulfate
BHI ..... brain heart infusion
B-ME ..... beta-mercaptoethanol
bp ..... base pair
BSA ..... bovine serum albumin
C ..... cytosine
cDNA ..... complementary DNA
CFU ..... colony forming unit
CRA ..... Congo red agar
Cm ..... chloramphenicol
Cm^r ..... chloramphenicol resistance
DNA ..... deoxyribonucleic acid
dNTP ..... deoxynucleotide triphosphate
DTT ..... dithiothreitol
E. coli ..... *Escherichia coli*
EDTA ..... ethylenediamine tetraacetic acid
EMSA ..... electrophoretic mobility shift assay
Erm ..... erythromycin
Erm^r ..... erythromycin resistance
g ..... gram
G ..... guanine
gDNA ..... genomic DNA
ica ..... intercellular adhesin
IPTG ..... isopropyl β-D-1-thiogalactopyranoside
kb ..... kilobase pairs
kDa ..... kilodalton
L ..... liter
LB ..... Luria-Bertani
M ..... molar
max ..... maximum

Mb ..... megabase
MIC ..... minimum inhibitory concentration
ml ..... milliliter
mM ..... millimolar
mRNA ..... messenger RNA
MRSA ..... methicillin resistant *Staphylococcus aureus*
MSSA ..... methicillin sensitive *Staphylococcus aureus*
MW ..... molecular weight
MWCO ..... molecular weight cut off
nM ..... nano molar
nm ..... nano meter
nmol ..... nano mol
OD ..... optical density
PBS ..... phosphate buffered saline
PBST ..... PBS supplemented with 0.05% Tween 20
PCR ..... polymerase chain reaction
PNAG ..... poly-N-acetylglucosamine
PVDF ..... polyvinylidene fluoride
RNA ..... ribonucleic acid
rpm ..... revolutions per minute
RT ..... reverse transcriptase
RT-PCR ..... reverse transcriptase PCR
S. aureus ..... *Staphylococcus aureus*
S. epidermidis ..... *Staphylococcus epidermidis*
sarA ..... Staphylococcal accessory regulator A
SDS ..... sodium dodecyl sulphate
SOC ..... super optimal broth
T ..... thymine
TAE ..... tris-acetate EDTA buffer
TBE ..... tris-borate EDTA buffer
TEMED ..... tetramethylenediamine
Tet ..... tetracycline
Tet^r ..... tetracycline resistance
TSA ..... tryptic soy agar
TSB ..... tryptic soy broth
TSBG ..... TSB supplemented with 1% glucose
U ..... uracil
UV ..... ultraviolet
VCU ..... Virginia Commonwealth University
V ..... volt
Wt ..... wild-type

Abstract

CHARACTERIZATION OF THE EXPRESSION OF THE INTERCELLULAR ADHESIN LOCUS IN *STAPHYLOCOCCUS AUREUS*

By: Jamie L. Brooks, Ph.D.

A dissertation submitted in partial fulfillment of the requirements for the degree of Doctor of Philosophy at Virginia Commonwealth University.

Virginia Commonwealth University
2012

Major Director: Kimberly K. Jefferson, Ph.D.
Associate Professor, Department of Microbiology and Immunology

Poly-N-acetylglucosamine (PNAG) is an important *Staphylococcus aureus* virulence factor. It is a major component of the extracellular polymeric matrix in biofilms, and contributes to resistance to the innate immune response. The proteins encoded in the *icaADBC* (intercellular adhesin) operon are responsible for PNAG production. Here, we present evidence of a new mechanism of phase variation for switching off PNAG production that involves slipped strand mutagenesis, along with further insight into the regulation and expression of the *icaADBC* operon. *S. aureus* strain MN8m (mucoid) is a

spontaneous mutant of strain MN8 (non-mucoid). It is characterized by constitutive overproduction of PNAG, resulting from a 5 bp deletion in the *icaADBC* promoter region. First, we explored the effect of this mutation on the binding of the positive regulator SarA and its regulation of *icaADBC* in MN8m; and demonstrated that while binding is not inhibited by the MN8m promoter mutation, it appears that SarA exhibits a negative influence on transcriptional activation in this strain background. Second, we found that non-mucoid mutants were frequently detected in MN8m cultures. The PNAG mutants still exhibited elevated *icaADBC* transcript levels and the 5 bp deletion was still present, but they were PNAG-negative. The most frequent mutation responsible for the phenotype was a slipped strand mispairing in the *icaC* gene. We found that, *in vitro*, PNAG-negative mutants had a growth advantage and increased fitness relative to the mucoid, PNAG-overproducing strain. Therefore, the slipped strand mutants in the PNAG-off state had a competitive growth advantage and eventually predominated the culture. Reversion back to mucoid occurred but revertants were isolated infrequently, due to their compromised fitness. The region of slipped strand mispairing was found to vary in several clinical *S. aureus* isolates, indicating *in vivo* relevance of this new mechanism. Third, a non-mucoid variant was isolated with the same phenotype and growth properties that instead had a nonsense mutation in *icaB*, which has demonstrated that there is a polar translational relationship between *icaB* and i*caC*. Together, these studies have given us insight into the regulation and expression of *icaADBC* expression and have revealed a growth disadvantage associated with PNAG overproduction.

CHAPTER 1

Introduction

Clinical Significance of *Staphylococcus aureus*

Staphylococcal bacteria are Gram-positive cocci that are part of the family Staphylococcaceae in the order Bacillales. The staphylococci are non-motile, non-spore forming facultative anaerobes, capable of growth by either aerobic respiration or fermentation. Staphylococci are oxidase negative and predominantly catalase positive, allowing them to be distinguished from streptococci. *Staphylococcus aureus* and *Staphylococcus epidermidis* are the most studied and well-characterized species of the genus. *Staphylococcus aureus* is of particular clinical importance because it is a major opportunistic pathogen responsible for a large range of infections that contribute significantly to morbidity, mortality and healthcare costs. It can be found commensally on mucosal surfaces such as the anterior nares, and transiently on the skin. *S. aureus* is a leading cause of nosocomial infections, particularly on indwelling medical devices. Infections occur when the bacteria cross the epithelial boundary, where they are capable of infecting a wide variety of body tissues. Mild soft tissue skin infections caused by *S. aureus* such as impetigo and foliculitis are generally self-limiting. However, more severe life-threatening infections including osteomyelitis, bacteremia, toxic shock syndrome, necrotizing pneumonia and infective endocarditis are commonly

caused by *S. aureus*. In fact, in the United States and Canada, *S. aureus* is the most common cause of skin/soft tissue infection, bacteremia, and nosocomial lower respiratory tract infections (Diekema *et al.*, 2001). Additionally, deaths from methicillin resistant *S. aureus* (MRSA) alone exceed 18,000 yearly in the United States, making it the leading cause of death by a single infectious agent (DeLeo & Chambers, 2009). Treatment of *S. aureus* infections is complicated by its tendency to acquire resistance to the antibiotics commonly used to combat infection, quickly becoming multi-drug resistant. Oxacillin/methicillin resistance (MRSA) is widespread in both hospital and community settings, with numerous vancomycin resistant (VRSA) strains already emerging as well (DeLeo & Chambers, 2009, Howden *et al.*, 2010). In 2010, *S. aureus* was reported to have acquired resistance to some of the newest antibiotics approved as last resorts for treatment, daptomycin and linezolid (Nannini *et al.*, 2010). *S. aureus* expresses an arsenal of virulence factors that allow it to establish infection and survive challenge. It can produce proteins and polysaccharides that inhibit complement and opsonization, as well as toxins, proteases, and superantigens (Foster, 2005). *S. aureus* also encodes various adhesion proteins/polysaccharides, and its ability to form a hardy/adherent biofilm can contribute to virulence. This proficient biofilm formation is associated with medical implant infections, although biofilm-associated infections can also be associated with host tissue. Examples of staphylococcal biofilm-associated infections include but are not limited to chronic rhinosinusitis, acute septic arthritis, endophthalmitis, chronic bacterial prostatitis, and native-valve endocarditis.

Biofilms

A biofilm is an aggregation of sessile bacteria that are encased in a predominantly self-produced extracellular polymeric substance/matrix (EPS) that holds them together and onto a surface. The extracellular polymeric matrix can be composed of bacterial proteinaceous adhesins, teichoic acids, extracellular DNA, and/or polysaccharides (Cucarella *et al.*, 2001, Izano *et al.*, 2008, Gross *et al.*, 2001). The ratio of these different EPS components is highly variable, changing in response to various stimuli; and can vary between different sites of infection or within a single biofilm at different points in time. The exact process of biofilm formation is difficult to define since different environmental conditions and bacterial genetic backgrounds can influence the function of numerous regulators, adhesins, and enzymes, causing a large degree of variation in physical characteristics. Cell-cell communication (quorum sensing) is optimized within a biofilm, since cells are held together closely, permitting coordinated gene expression and maturation of the biofilm over time (Davies *et al.*, 1998).

Initial adherence of planktonic bacteria to a surface begins the process of biofilm growth, when cells begin deposition of the EPS molecules encouraging intercellular aggregation. As a biofilm matures it develops a distinct physical architecture to maintain hydration and the flow of nutrients to the resident bacteria that is characterized by tower-like structures interspersed with fluid-filled channels (Costerton *et al.*, 1995). As a biofilm becomes fully mature, individual planktonic cells or small clumps of intact biofilm may be dispersed into the surrounding environment to seed new sites of infection.

The biofilm mode of growth confers several different survival advantages on the resident bacteria, including a high degree of resistance to environmental forces like UV light, sheer force, and desiccation. The biofilm is also capable of shielding cells from the host immune response (Vuong *et al.*, 2004b) and challenge with numerous different types of antibiotics. In fact, biofilm bacteria are able to withstand antibiotic concentrations up to 1000-fold higher than their genetically identical planktonic counterparts (Hoyle & Costerton, 1991). Several different aspects of biofilm formation have been suggested to contribute to these significant survival advantages. Biofilms are organized into different regions of altered metabolic activity based upon the availability of nutrients and external stimuli. Bacteria tend to become less aerobic and growth is slowed as proximity from the edges of the biofilm diminish, resulting in a sub-population of cells that are intrinsically resistant to antibiotics that depend on active cellular growth for their mode of killing (Brown *et al.*, 1988). This resistance effect is heightened by the extrapolymeric matrix surrounding the cells within a biofilm. The EPS molecules at the biofilms exterior perimeter may slow penetration of a certain antimicrobials through electrostatic properties or size/physical properties, depleting the local lethal concentration and/or allowing more time for cells further within the biofilm to react (Vuong et al., 2004b, Walters *et al.*, 2003). Additionally, recent evidence points to increased concentration of a sub-population of persister cells within biofilms (Keren *et al.*, 2004). Persister cells are dormant cells that are highly tolerant to a variety of antibiotics, and they are capable of reestablishing a biofilm infection after even extremely high concentrations of antimicrobials that have been applied are removed, complicating complete eradication of a biofilm infection and leading to relapse. Biofilm-

mediated resistance is a phenotypic trait, and if an established biofilm can be successfully dispersed the bacteria regain planktonic levels of sensitivity to antibiotics and to host immune defenses.

Staphylococcal Biofilms

A wide variety of extracellular adhesive matrix components have been identified as mediators of staphylococcal biofilms. Extracellular DNA, either derived from lysed bacteria or potentially from other sources (such as DNA released by neutrophils during host immune response), has been shown to be a major component of staphylococcal biofilm extracellular matrix, particularly in *S. aureus* biofilms (Izano *et al.*, 2008). *Staphylococcus aureus* also expresses a large variety of surface-associated proteinaceous adhesins that can contribute to the composition of the EPS. Additionally, other surface expressed proteins can play a role, including different MSCRAMMs (microbial surface components recognizing adhesive matrix molecules), such as fibronectin-binding proteins (FnbpA, FnbpB), collagen-binding protein, clumping factors (ClfB), and SasG. Polysaccharide adhesins can also mediate biofilm formation, and one of the most prominent and well-characterized adhesive molecules in *S. aureus* infections is the polysaccharide poly-N-acetylglucosamine.

***icaADBC* and Poly-N-acetylglucosamine**

A major component of the *S. aureus* biofilm extracellular matrix, and an important virulence determinant in *S. aureus* infections in general, is the polysaccharide poly-N-acetylglucosamine. Poly-N-acetylglucosamine (PNAG), also referred to as

polysaccharide intercellular adhesin (PIA) in *S. epidermidis*, is a high molecular weight polymer of **β**-1-6-linked N-acetyl-glucosamine (Mack *et al.*, 1996, Maira-Litran *et al.*, 2002). In addition to its role in intercellular adhesion and biofilm formation, PNAG also plays a role in immune evasion (Cerca *et al.*, 2007, McKenney *et al.*, 1998). PNAG is synthesized by the proteins encoded in the *icaADBC* intercellular adhesin locus (Fig. 1 & 2). IcaA is a transmembrane glucosyltransferase that, together with IcaD, produces short PNAG oligomers (Gerke *et al.*, 1998). IcaC is an integral membrane protein that is necessary for linking the short oligomers into longer polymer chains, and is thought to be involved in translocation of these chains to the cell surface (Gerke et al., 1998). Once there, IcaB is responsible for partial deacetylation of the PNAG molecule, which is required for retention at the cell surface (Vuong *et al.*, 2004a). There are multiple known regulators of the *ica* locus. The *icaR* gene is located upstream of the *icaADBC* operon. It is a direct transcriptional repressor that is divergently transcribed from the rest of the operon. CodY has also been demonstrated to act as a negative transcriptional regulator (Majerczyk *et al.*, 2008). The *S. aureus* global regulator SarA is an important positive regulator of *ica* that has been shown to bind in and around its promoter region (Tormo *et al.*, 2005).

***Staphylococcus aureus* strain MN8m**

S. aureus strain MN8m has proven to be a useful tool for investigating the role of PNAG is biofilm formation, due to its defining characteristic as a PNAG over-producing strain. MN8m was originally isolated as a spontaneous mutant by virtue of its mucoid phenotype from a chemostat culture of strain MN8, a toxic shock syndrome clinical

isolate (Cramton *et al.*, 1999). The mutation that conferred this PNAG-overexpression, or the mucoid phenotype, was identified as a 5-bp deletion in the *icaADBC* promoter

Figure 1: Organization of the *icaADBC* operon. The Ica proteins are encoded by the *icaADBC* locus, which includes the divergently transcribed *icaR* gene.

Figure 2: Roles of *IcaADBC* in PNAG synthesis. The exopolysaccharide poly-N-acetylglucosamine (PNAG) is synthesized by the Ica proteins. (1) IcaA, a transmembrane glucosyltransferase, assembles short PNAG oligomers in conjunction with the IcaD membrane protein. (2) The PNAG precursors are then assembled into growing polymer chains by the transmembrane protein IcaC, which is thought to then translocate them to the cell surface. (3) IcaB is located on the cell surface and is responsible for partial deacetylation of the PNAG molecule, introducing random positively charged regions to the polymer, allowing it to be surface retained.

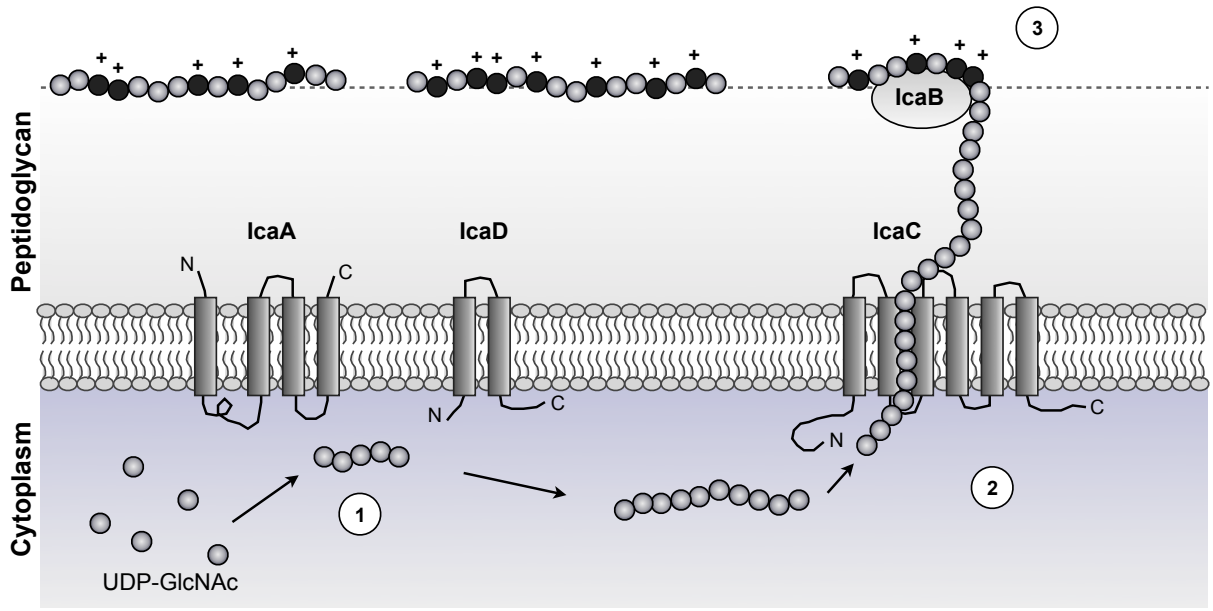

Figure 3. Schematic representation of the promoter region of the MN8 *ica* operon. Promoter elements, effector binding sites, and transcriptional start sites (TSS) are labeled. The five nucleotides underlined in purple at the TSS of *icaR* represent the 5 bp deleted in the mutation from MN8 to MN8m, previously identified as responsible for the conversion.

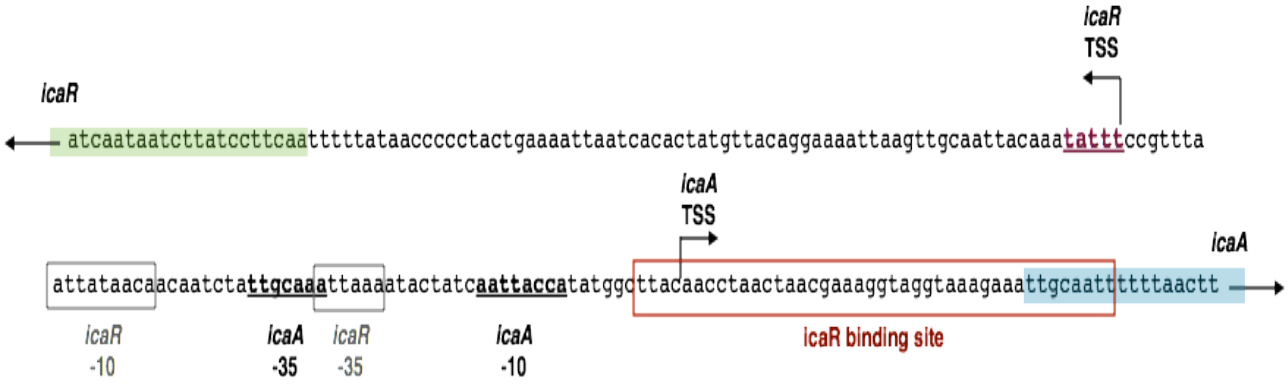

region (Jefferson *et al.*, 2003) (Fig. 3). The mutation leads to constitutive *icaADBC* transcription, but the molecular basis for this overexpression has not been defined. Preliminary evidence shows that the effect is not mediated by interference of the deletion with the transcriptional start site of the divergently transcribed negative regulator IcaR, since the complete absence of *icaR* does not stimulate *icaADBC* transcription to the extent that is observed in strain MN8m.

Research Objectives

Staphylococcus aureus infections are of particularly important clinical significance due their widespread nature, enormous expense associated with treatment, and high morbidity and mortality. The ability of *S. aureus* to rapidly develop antibiotic resistance has led to the pursuit of alternative therapeutic approaches. Recent recognition of the major role that biofilm formation plays in many *S. aureus* infections has made it a major target of interest for new treatment development. Many of the proposed anti-biofilm therapies focus on inhibition, reversal, or dispersal of the biofilm phenotype by targeting the extracellular polymeric matrix. In order for this to be a viable new approach to treatment, our understanding of how the adhesive molecules that make up the EPS matrix are regulated, must be expanded and improved. Although the role of PNAG in *S. aureus* biofilms as an adhesin has been well established, our knowledge about its regulation remains incomplete. The goal of this project is to utilize a strain that over-produces PNAG to better elucidate details of the expression and regulation of the *icaADBC* operon responsible for PNAG synthesis. First, to better

understand promoter-regulator interactions and promoter characteristics that influence transcriptional activation. Secondly, to explore new evidence that PNAG expression can be modulated by phase variation within a biofilm population to reduce its contribution. These objectives have resulted in characterization of a novel form of phase variation PNAG that suggests a potential for roles of the *icaADBC* genes beyond PNAG synthesis, and the realization of a previously unknown polar relationship between genes of the operon. This study also provides new insight into the role of SarA in *icaADBC* activation, and further characterization of the molecular mechanism responsible for over-production of PNAG in *S. aureus* strain MN8m.

CHAPTER 2

Materials and Methods

Staphylococcal strains and culture conditions. Bacterial strains used in these studies are listed in **Table 1**. *Staphylococcus aureus* strains were grown aerobically at 37°C on tryptic soy agar (TSA) plates containing the appropriate antibiotic. Liquid cultures were in tryptic soy broth containing 1% glucose (TSBG), incubated aerobically at 37°C, 200 rpm. Congo red agar, used to asses mucoid phenotype by colony morphology, was composed of brain heart infusion (BHI) agar + 3.6% sucrose + 0.5% glucose + 0.08% Congo red. *Escherichia coli* strains were grown aerobically at 37°C on Luria-Bertani broth (LB) agar plates containing the appropriate antibiotic. *E. coli* liquid cultures were in LB, incubated aerobically at 37°C, 200 rpm. Appropriate antibiotics were incorporated at the following concentrations: 100 µg/ml ampicillin (Amp) for *E. coli*, 35 µg/ml chloramphenicol (Cm) for *E. coli*, 10 µg/ml Cm for *S. aureus*, 5 µg/ml tetracycline (Tet) for *S. aureus*, and 10 µg/ml erythromycin (Erm) for *S. aureus*.

Agarose gels. 1.0% agarose gels were prepared by dissolving agarose in 1X Tris-acetate-EDTA (TAE) buffer (Fisher Scientific, Pittsburg, PA), with 0.15 µg/mL ethidium bromide added before pouring. 10X BlueJuice loading buffer (Invitrogen, Grand Island, NY) was added to DNA samples to achieve a 1X final concentration. Gels were run

Table 1. Bacterial strains

S. aureus Strains	Description	Source
MN8	Nonmenstrual toxic shock syndrome clinical isolate	(Schlievert & Blomster, 1983)
MN8Δ*ica::tet*	*icaRADBC* mutant of *S. aureus* MN8 (Tet^r)	(Jefferson et al., 2003)
MN8Δ*sarA::erm*	*sarA* mutant of *S. aureus* MN8 (Erm^r)	Jefferson lab strain
MN8m	Spontaneous mucoid mutant isolated from a chemostat culture of *S. aureus* MN8	(Cramton et al., 1999)
JB12	Spontaneous non-mucoid mutant isolated from a chemostat culture of *S. aureus* MN8m	This study
JB12 + pCL15	Complementation of JB12 with pCL15 (Cm^r, empty vector)	This study
JB12 +pCL15-*icaC*	Complementation of JB12 with *icaC* from MN8m *in trans* using pCL15 (Cm^r) Primers: icaCSphIFwd, icaCKpnIRev	This study
JB17	Spontaneous non-mucoid mutant isolated from a chemostat culture of *S. aureus* MN8m	This study
JB17 + pCL15	Complementation of JB17 with pCL15 (Cm^r, empty vector)	This study
JB17 + pCL15-*icaB*	Complementation of JB17 with *icaB* from MN8m *in trans* using pCL15 (Cm^r) Primers: icaBBamHIFwd,icaBEcoRIRev	This study
JB17 + pCL15-*icaC* (native)	Complementation of JB17 with *icaC* from MN8m *in trans* using pCL15 (Cm^r) Primers: icaCSphIFwd, icaCKpnIRev	This study
JB17 + pCL15-*icaC* (ideal)	Complementation of JB17 with *icaC* from MN8m with a modified ribosomal binding site, *in trans* using pCL15 (Cm^r) Primers: icaCRBSFwd, icaKpnIRev	This study

JB17 + pCL15-*icaBC*	Complementation of JB17 with *icaBC* from MN8m *in trans* using pCL15 (Cm^r) Primers: icaBSphIFwd, icaCKpnIRev	This study
ALC1342Δ*sarA::erm*	*sarA* mutant of *S. aureus* RN6390 (Erm^r)	(Cheung & Manna, 2005)
RN4220	Restriction defective derivative of *S. aureus* RN450	(Kreiswirth *et al.*, 1983)
RN4220Δ*ica::tet*	*icaRADBC* mutant of *S. aureus* RN4220 (Tet^r)	Jefferson lab strain
RN4220Δ*ica*::tet + pBT9-M1	Complementation of RN4220 *icaADBC* mutant with i*caRADBC* from MN8m *in trans* using pBT9 (Tet^r, Cm^r)	This study
RN4220Δ*ica*::tet Δ*sarA::erm* + pBT9-M1	Complementation of RN4220 *sarA* and *icaRADBC* mutant with i*caRADBC* from MN8m *in trans* using pBT9 (Tet^r, Cm^r)	This study

***E. coli* Strains**	**Description**	**Source**
CH3 Blue	Chemically competent cells derived from *E. coli* K12, cloning strain (Amp^r when transformed with plasmid)	Bioline (Tauton, MA)
BL21-CodonPlus(DE3)-RIL	Chemically competent cells derived from E. coli BL21, heterologous protein expression strain (Amp^r when transformed with plasmid, Cm^r)	Stratagene (La Jolla, CA)
BL21 + pET32xT-*sarA*	BL21-CodonPlus(DE3)-RIL cells containing *sarA* from MN8 *in trans* using pET32xT (Amp^r, Cm^r)	This study

at 125 volts in 1X TAE buffer and visualized under UV light. DNA size was determined by comparison against the Hyperladder series of DNA molecular weight markers (Bioline, Taunton, MA).

Biofilm growth assay. Microtiter plate assays for biofilm formation were performed essentially as described previously by Christensen *et al*. (1985) with minor modifications. Cultures were grown overnight in 4 ml of TSBG or TSBG + 10 µg chloramphenicol/ml, diluted 1:200 in the same media or media with 1mM IPTG added for plasmid induction, and aliquoted into 96-well polystyrene flat-bottom microtiter plates (Greiner Bio-One, Monroe, N. Carolina). After 24 hours at 37°C, the wells were emptied and washed once with phosphate-buffered saline (PBS). The plates were dried at room temperature, stained with 200 µl safranin for 1 minute, washed gently with water, and allowed to dry. The biofilms were assessed qualitatively by visual inspection and images were taken using a digital scanner. The safranin was then resuspended in 200 µl 33% acetic acid and the wells were analyzed by spectrophotometry at $OD_{562\ nm}$ using a 96-well plate spectrophotometer.

Planktonic growth assay. To generate a bacterial growth curve, cultures were grown overnight in TSBG, and gently sonicated for 30 seconds. Each culture was diluted to OD_{600nm} of 0.1 and used to inoculate fresh TSBG 1:100, with separate tubes for each time point. The cultures were incubated at 37°C, 200 rpm. At each time point the cultures were gently sonicated, the OD_{600nm} measured, and then serially diluted and

plated in triplicate on TSA plates to determine the number of colony forming units (CFU).

gDNA extraction. To isolate genomic DNA, bacteria were grown overnight in liquid cultures, diluted to OD_{600nm} = 1.0 in 1 ml total volume, and collected by centrifugation. The bacterial pellets were resuspended in 180 µl of lysis buffer, composed of 2.4 µl Triton X-100, 10 µl 5 mg/ml lysostaphin, and 20 mg lysozyme in 190 µl 1X TE buffer (10 mM Tris-HCl pH 7.5, 1 mM EDTA); and incubated for 30 minutes at 37°C. The Qiagen DNeasy Blood and Tissue kit (Qiagen, Valencia, CA) was used from this point to extract the gDNA. Samples were incubated with 25 µl proteinase K and 200 µl Buffer AL at 56°C for 30 min, and 200 µl 100% ethanol added. The mixture was transferred to DNeasy Mini spin column, centrifuged at max speed for 1 minute, and the column was then washed with 500 µl Buffer AW1. After repeating centrifugation, 500 µl Buffer AW2 was added and the column dried by centrifugation at max speed for 3 minutes. gDNA was eluted by application of 200 µl sterile water directly to the column membrane, followed by centrifugation for 1 minute.

Polymerase chain reaction (PCR) and product purification. Similar general conditions were used for all PCR amplification of DNA with slight modifications dependent on the DNA template to be used, product size, or the melting temperature (T_M) of the primer set. Reaction mixtures were typically 50 µl total volume composed of 10 µl 5X Phire buffer (Thermo Scientific, Waltham, MA), 1.5 µl 10mM dNTPS (2.5 mM of each), 10 pmol of both the forward and reverse primers, DNA template and 1 µl Phire II

polymerase in sterile water. For reactions using gDNA as template 3 µl was added; whereas only 1 µl was used for reactions based on plasmid DNA or DNA products purified from previous PCR's. Template material for colony PCR was obtained by resuspended a single colony in 10 µl sterile water, and using 3 µl of the mixture for the reaction. Reaction conditions were programmed into a thermal cycler machine as: hot start at 105°C, initial denaturation at 95°C for 2 minutes, followed by 35 cycles of 94°C for 30 seconds, T_M + 3°C of the lower primer T_M for 30 seconds, and 72°C for 15 seconds per kb of expected product size, and a round of final extension at 72°C for 10 minutes. PCR products were purified after electrophoresis in agarose gel using the QIAquick Gel Extraction kit (Qiagen, Valencia, CA) as described by the manufacturer.

Plasmid DNA purification and manipulation. Plasmid purifications were performed using the QIAprep Spin Miniprep kit (Qiagen, Valencia, CA) according to the manufacturer's instructions, from overnight cultures of *E. coli* single colony transformants in 3 ml LB with ampicillin. All restriction enzymes, specific buffers, and BSA used for restriction enzyme digests of plasmid DNA or PCR products were purchased from New England Biolabs (Ipswich, MA), and used according to the manufacturer's recommendations. After plasmid restriction digestion, the 5' phosphoryl groups were removed using Antarctic Phosphatase and its supplied buffer (New England Biolabs, Ipswich, MA) according to manufacturer's instruction, to prevent re-ligation. Ligation of DNA fragment inserts into digested plasmids was accomplished using Ready-To-Go T4 DNA Ligase and Ligase Buffer (Amersham Biosciences, Piscataway, NJ) at roughly a 3:1 ratio of insert to plasmid, at 16°C for a minimum of 1 hour.

Table 2. Primer List

Primer Name	Sequence
icaseq1	5'-CAAGTGTTGTACCGTCATACC-3'
icaseq2	5'-CGTCGATTTACAAGAAAACAGAGG-3'
icaseq3	5'-AGGTCTTTGGAAGCAACGCG-3'
icaseq4	5'-ATCGCTATATCTTGTGTCTTTTGG-3'
icaseq5	5'-AAATGGCTAAAATCACATGATGC-3'
icaseq6	5'-TACCGGTAATCAAAAAAGCTGGG-3'
icaseq7	5'-GTCCTATTAGGTCAATGGTATGG-3'
icaseq8	5'-GAGGATAATACAATGGTCTTTCTAGC-3'
icaseq9	5'-CACTCCCATTGGCATTTACGAAG-3'
icaseq10	5'-CCAATAGTCTCCATTTGCTAACGC-3'
icaseq11	5'-ACGCGTGTAGTTAAGTATCTATAGG-3'
icaseq12	5'-GATAAGTTATGCAAATCGTGGGTATG-3'
icaseq13	5'-ACCATCCAGTGTGCTTACAGG-3'
icaseq14	5'-GCGACTATCAATAAAGAGTGCGACTG-3'
icaseq16	5'-CCAGCAAGTGTCTGACTTCG-3'
icaseq16	5'-CATCCACATTTATGTCAGGCTTC-3'
sarAFwd	5'-CGCGGATCCGCAATTACAAAAATCAATGATT-3'
sarARev	5'-GGGCTCGAGTTATAGTTCAATTTCGTTGTT-3'
icaBBamHIFwd	5'-CCGCGGATCCCAAAAATGGCAGAGAGGAAGA-3'
icaBEcoRIRev	5'-CCGCGAATTCAGCACGTAAATATACGAGTTCAAGT-3'
icaBSphIFwd	5'CCGCGCATGCCAAAAATGGCAGAGAGGAAGA-3'
icaCSphIFwd	5'-CCGCGCATGCCAAAAATGGCAGAGAGGAAGA-3'
icaCKpn1Rev	5'-CCGCGGTACCCCGCGTGTTTTTAACATAGC-3'
icaCRBSFwd (SphI)	5'-CCGCGCATGCGAGCATTTAATTAAGAGATGAGGAGGATTC-3'

16SRTFwd	5’- TATGCATCGTTGCCTTGGTA-3’
16SRTRev	5’-GAACCGCATGGTTCAAAAGT-3’
icaCRTFwd	5’-CGAACAACACAGCGTTTCAC-3’
icaCRTRev	5’-CGTTCCAATAGTCTCCATTTGC-3’
icaRRTFwd	5’-TTTGTAATTGCAACTTAATTTTCCTG-3’
icaRRTRev	5’-AAACAACATTTAACACTTTGTTCGT-3’
sarARTFwd	5’-TTGCTTTGAGTTGTTATCAATGG-3’
sarARTRev	5’-TTTCTCTTTGTTTTCGCTGATG-3’
icaProBTFwd	5’-TGTTACAGGAAAATTAAGTTGCAATTACA-3’
icaProBTRev-BioTEG	5’-GGTTGTAAGCCATATGGTAATTGATAGT-3’
icaProBend1-Xba	5’-TCTAGACTATGTTACAGGAAAATTAAGTTGC-3’
icaProBend2-Sal	5’-GTCGACGATAGTATTTTAATTTGCAATAGATTGTTG-3’

Transformation of chemically competent E. coli. One vial of chemically competent *E. coli* cells was thawed on ice; 4 µl of plasmid ligation reaction was gently added and incubated on ice for 30 minutes. The tube was transferred to a 42°C water bath for 30 seconds, and placed back on ice until 200 µl SOC media (85.5 mM NaCl, 2.5 mM KCl, 10 mM $MgCl_2$, 2% tryptone, 0.5% yeast extract, and 20mM glucose) could be added. The cells were allowed to recover at 37°C for 1 hour, and then plated on LB plates with appropriate antibiotic selection.

Production of electrocompetent S. aureus *RN4220.* Overnight cultures of *S. aureus* RN4220 were grown shaking in TSB at 37°C, 200 rpm. The bacteria were subcultured by 1:100 dilution in fresh TSB, and grown to exponential phase (OD_{600nm} = 0.5 to 0.8) at 37°C, 200 rpm. Cell pellets were obtained by centrifugation for 15 minutes at 4°C, 4000 rpm. All subsequent steps were carried out on ice, with pre-chilled reagents. The pellet was washed three times with 25 ml of ice cold sterile water, using 5 minute centrifugations to re-pellet cells in between washes. The pellet was then washed a final time in 30 ml cold 10% glycerol in water, before being resuspended in 15 ml 10% glycerol and incubated at room temperature for 15 minutes. The cells were then again collected by centrifugation, and the final pellet resuspended in 500 µl 10% glycerol. Aliquots (50 µl) were stored at -80°C until use.

Transformation of electrocompetent S. aureus. One vial of electrocompetent *S. aureus* RN4220 cells was thawed on ice; 5 µl plasmid DNA was gently added and incubated on ice for 30 minutes. The mixture was then transferred to an electroporation cuvette with a

gap length of 0.1 cm and pulsed once using the Micropulser machine (Bio-Rad, Hercules, CA) pre-set *S. aureus* setting (1.8 kV, 2.5 msec, 25 μF). Immediately following electroporation, 500 μl of TSB containing the appropriate antibiotic (diluted 1:500 from normal liquid culture concentration to a sub-inhibitory concentration) was added and the entire mixture transferred to a culture tube. The cells were allowed to recover at 37°C for 2 hours, and then plated on TSA plates with appropriate antibiotic and incubated overnight at 30°C.

Phage transduction. The generalized transducing phage 80α was used to create allelic exchange mutants or to move plasmids between *S. aureus* strains. The donor strain was scraped from an overnight plate into 250 μl TSB until extremely turbid, which was then added to 0.4% soft TSA containing 5 μl of 2 M $CaCl_2$. After addition of 75 μl of phage 80α, the mixture was poured onto a TSA plate and incubated at 37°C until lysis occurred, indicated by clearing of the top agar. Following lysis, the soft top agar was collected, centrifuged, and the supernatant filter sterilized using a 0.45 μm syringe filter. The recipient strain was scraped from an overnight plate into 300 μl TSB until extremely turbid, and was divided into three 100 μl culture tubes containing 2.5 μl of 2 M calcium chloride each. Aliquots of the phage lysate, either 75 μl, 150 μl, or 250 μl were added to each of the tubes and the total volumes brought up to 2 ml with TSB. The mixtures were incubated shaking at 37°C for exactly 20 minutes, and 3 ml of 20 mM sodium citrate added. After centrifugation to collect the bacteria, the pellet was resuspended in 3 ml sodium citrate again and centrifuged. The remaining pellet was resuspended in 500 μl

20 mM sodium citrate, incubated at 37°C for 2 hours, and then plated on TSA containing the appropriate antibiotic to be incubated for 48 hours at 37°C.

RNA isolation. Overnight liquid cultures were diluted 1:10 in 5 ml TSBG and incubated shaking for 4 hours at 37°C. The bacteria were collected by centrifugation and stored at -80°C, for a minimum of 1 hour or until use. RNA was extracted using the Qiagen RNeasy Mini kit (Qiagen, Valencia, CA) with some modifications. The pellets were resuspended in 500 µl Buffer RLT and transferred to 2 ml tubes containing 1mm glass beads (Research Products International Corp., Mount Prospect, IL). After adding 500 µl cold acid phenol, the cells were lysed twice using a FastPrep FP120 (Thermo, Pittsburgh, PA) at a speed setting of 6.0 for 40 seconds, cooling the tubes on ice for 5 minutes between the runs. The aqueous phase was collected after centrifugation and mixed with 500 µl 100% ethanol. Samples were applied to an RNeasy spin column, and following manufacturer's instructions, the column was washed once with 700 µl Buffer RW1 and twice with 500 µl Buffer RPE. The columns were dried by centrifugation at max speed for 3 minutes and the RNA eluted in 90 µl sterile, nuclease-free water. Contaminating DNA was digested with Turbo DNase (Ambion, Austin, TX) with the accompanying buffer for 1 hour at 37°C. The DNase was inactivated and removed using DNase Inactivation Reagent (Ambion) according to manufacturer's directions. Absorbance was measured at 260 nm and 280 nm using a NanoDrop 10000 (Thermo Scientific, Waltham, MA), and the ratio of the two values was used to calculate the concentration of RNA.

cDNA synthesis. cDNA was synthesized from 1 µg of isolated mRNA by a two-step reverse transcription reaction using the Bioline Tetro cDNA synthesis kit (Bioline, Tauton, MA) according to manufacturer's directions. The RNA was mixed with 10 pmol of up to six gene-specific reverse primers in 10 µl total volume, and incubated at 70°C for 10 minutes. 1 µl of 10mM dNTPs (2.5 mM of each), 1 µl RNase inhibitor, 4 µl 5X RT buffer, and 1 µl reverse transcriptase in 10 µl total volume was added to the RNA + primer mix. This was followed by incubation for 2 hours at 42°C, and 70°C for 15 minutes. Control reactions (noRT) contained only RNA and water.

Real-time RT-PCR. cDNA synthesized from isolated mRNA, or the noRT control, was diluted 1:10 in water for use with gene-specific primers, and 1:1000 for 16S reactions. The reaction mix was composed of 2 µl of the diluted cDNA, 10 pmol of both the forward and reverse primers, 8.5 µl sterile water, and 12.5 µl SYBER Green Sensimix (Bioline, Tauton, MA). Real-time RT-PCR was performed in a iQ5 Multicolor Realtime PCR Detection system (BioRad, Hercules, CA) following the programmed steps: 1 cycle of 3 minutes at 95°C, 40 cycles of 20 seconds at 95°C, 20 seconds at 55.2°C, 20 seconds at 72°C while collecting real time-PCR readings, and 41 cycles of 30 seconds at 55°C while collecting melting curve readings. Data was recorded in cycle threshold (Ct) for each sample in technical triplicate, and normalized to the 16S transcript level by calculating $2^{(16S\ Ct - Gene\ Ct)}$. Ratios were determined between normalized sample values to produce fold differences.

Poly-N-acetylglucosamine (PNAG) slot blot. PNAG slot blots were performed essentially as described previously by Cramton et al. (2001) with minor modifications. Bacteria were grown overnight in TSBG or TSBG + 10 µg chloramphenicol/ml + 1mM IPTG. For cell surface extracts 10^9 cells were collected by centrifugation, washed once with PBS, and resuspended in 250 µl of 0.5M ethylenediaminetetraacetic acid (EDTA). To analyze secreted PNAG, 250 µl of spent media was retained. All samples were incubated in boiling water for 5 minutes, cooled, and incubated at 65°C for 1 hour with 20 µl proteinase K. Samples were boiled for an additional 5 minutes to inactivate the protease, diluted in 1X PBS, and immobilized on a nitrocellulose membrane that was pre-wetted in 10% methanol in 1X-PBS with a vacuum manifold. The membrane was blocked overnight at 4°C in 5% bovine serum albumin diluted in 1X PBS, then probed with 1:5,000-diluted rabbit antiserum specific for PNAG (kindly provided Dr. Gerald B. Pier) (Maira-Litran *et al.*, 2002) in 1X PBS + 1-2% blocking solution + 0.05% Tween-20 (Fisher Scientific, Pittsburg, PA) for 2 hours at room temperature, while rocking. The membrane was washed three times for 5 minutes with 1X PBST (PBS + 0.05% Tween-20), and then probed with 1:10,000- diluted goat anti-rabbit immunoglobulin-horseradish peroxidase conjugate (Invitrogen, Grand Island, NY) in 1X PBST for 1 hour at room temperature, while rocking. Bands were visualized with the ECL Plus western blotting detection system (GE Healthcare). The blot was incubated in the chemiluminescence developing reagent for 1 minute, covered in plastic wrap, exposed to X-ray film and developed in an X-O-Mat.

Isolation of JB12 mucoid revertants. Six-well polystyrene plates (CellTreat, Shirley, MA) were inoculated with individual colonies of JB12 in LB, grown at 37°C for 3 days, replacing the media every 24 hours. To collect mucoid revertants the wells were washed once with sterile 1X PBS, remaining adherent cells were scraped from the surface of the well and resuspended in PBS. After plating on CRA, colony morphology was visually assessed to identify mucoid CFUs.

Fitness determination. Cultures were grown overnight in TSBG, and gently sonicated for 30 seconds. Each culture was diluted to a concentration of 10^3 cells and mixed 1:1 with MN8m + JB12, with separate tubes for each time point. The cultures were incubated at 37°C, 200 rpm. At each time point the cultures were gently sonicated, serially diluted and plated in triplicate on CRA plates for CFU counting. Calculation of the difference in fitness was determined using the function derived from Sander *et al.* (2002):

$$M_t = \ln\left[\left(\frac{nm_t/m_t}{nm_{t-1}/m_{t-1}}\right)^{1/gen}\right]$$

where nm_t and m_t represent the non-mucoid and mucoid cells, respectively at a given time *t*. While nm_{t-1} and m_{t-1} denote the quantity of non-mucoid and mucoid cells at the preceding time point. The quotient of the ratios was standardized with the exponent 1/generation, with the assumption that cell numbers determined at 24 hours represents approximately 17 generations. The relative bacterial fitness for a given time was calculated as $fit_t = 1 + M_t$. The fitness value is equal to 1 if there is no difference in

fitness between the competing strains, less than 1 if the non-mucoid phenotype reduces fitness, or greater than 1 if the non-mucoid phenotype increases bacterial fitness.

Cell survival in nutrient-limited conditions. Liquid cultures were initially grown shaking aerobically in TSBG for 24 hours at 37°C, 200 rpm. Bacteria were collected by centrifugation, and equal numbers of bacteria for each sample were resuspended in equal volumes of MOPS minimal media with no glucose, or other carbon source. The cultures were incubated at 37°C while shaking. At each time point the cultures were serially diluted and plated in triplicate on TSA plates for CFU enumeration. Each strain was analyzed in technical triplicate and biologic replicates.

Polyacrylamide gel electrophoresis. Protein gels were run using the NuPAGE SDS-PAGE Gel system (Invitrogen, Grand Island, NY) according to manufacturer's instructions with slight modifications. 100 µl of liquid cell culture was collected by centrifugation, resuspended in 50 µl sterile water, and mixed with 50 µl NuPAGE 4X LS Sample Buffer and 10 µl NuPAGE Sample Reducing Buffer (Invitrogen). Samples were incubated in boiling water for 5 minutes, gently sonicated, and loaded into the wells of NuPAGE 4-12% Bis-Tris 1.0 mm Gel (Invitrogen). The gel was electrophoresed for approximately 30 minutes at 200 V in 1X NuPAGE Running Buffer. Approximate protein size was determined by comparison against Precision Plus Protein Kaleidoscope standard (BioRad, Hercules, CA). Lanes were visualized by staining with Imperial Protein Stain (Thermo Scientific, Waltham, MA) for 1 hour, and destaining with water until bands were clearly visible.

Western blot to detect 6X-His-tagged proteins. A 0.45 µm PVDF membrane (Invitrogen, Grand Island, NY) was pre-wetted in 100% methanol, then soaked in 1X NuPAGE transfer buffer (Invitrogen) containing 10% methanol along with transfer paper and sponges. Following polyacrylamide gel electrophoresis, the gel was prepared for electrophoretic transfer by rinsing in deionized water and then placed against the PVDF membrane; surrounded by the transfer paper and sponges to maintain buffer saturation and tight contact between the membrane and gel, and immersed in the same 1X NuPage transfer buffer. The transfer was run at 40V for 1 hour at room temperature. The membrane was blocked overnight at 4°C in 5% skim milk diluted in 1X PBS, then probed with 1:1,000-diluted rabbit anti-6X HIS Tag primary antibody (Rockland Immunochemcials, Gilbertsville, PA) in 1X PBS + 1-2% blocking solution + 0.05% Tween-20 (Fisher Scientific, Pittsburg, PA) for 2 hours at room temperature, while rocking. The membrane was washed three times for 5 minutes with 1X PBST (PBS + 0.05% Tween-20), and then probed with 1:10,000- diluted goat anti-rabbit immunoglobulin-horseradish peroxidase conjugate (Invitrogen, Grand Island, NY) in 1X PBST for 1 hour at room temperature, while rocking. Bands were visualized with the ECL Plus western blotting detection system (GE Healthcare). The blot was incubated in the chemiluminescence developing reagent for 1 minute, covered in plastic wrap, exposed to X-ray film and developed in an X-O-Mat.

Production of recombinant SarA. The primer set sarAFwd (BamHI site) and sarARev (XhoI site) were used to PCR amplify *sarA* from MN8 gDNA with directional restriction

sites on either end of the PCR product. After gel electrophoresis and purification by gel extraction, the PCR product was restriction digested with BamHI and XhoI (New England Biolabs, Ipswich, MA) according to manufacturer's specification. The isopropyl β-D-1 thiogalactopyranoside (IPTG) inducible plasmid pET32xT was also digested with BamHI and XhoI, prior to ligation of the digested *sarA* insert into the vector. The plasmid construct was used to transform chemically competent *E. coli* CH3 blue cells (Bioline, Tauton, MA) with transformants being selected for on LB agar plates containing ampicillin. The plasmid construct was isolated using the previously outlined plasmid mini-prep procedure, and the sequence fidelity of the gene insert confirmed by nucleotide sequencing. The pET32xT-sarA construct was then used to transform chemically competent *E. coli* BL21-CodonPlus(DE3)-RIL cells (Stratagene, La Jolla, CA), with transformants being selected for on LB agar plates containing ampicillin and chloramphenicol.

To induce expression of recombinant SarA, a streak of many BL21+pET32xT-*sarA* colonies was used to inoculate 50 ml of LB containing ampicillin and chloramphenicol, which was incubated shaking overnight at 37°C. The entire overnight culture was then transferred into 1 L of LB containing ampicillin and chloramphenicol, and incubated shaking at 37°C for 2 hours. A 1 ml aliquot was removed and saved prior to induction with 1 mM IPTG for 2 hours at 37°C. After protein induction, another 1 ml aliquot was removed and the entire remaining culture centrifuged to collect the bacterial cells. The pellet was washed once in sterile PBS, and frozen at -80°C for a minimum of 1 hour. To confirm proper protein expression, the pre- and post-induction samples were run on a polyacrylamide gel as previously described, stained and visualized.

Purification of recombinant SarA. The induced BL21+pET32xT-*sarA* pellet was resuspended in lysis buffer on ice, and sonicated six times for 30 seconds at power level 5 while remaining on ice. Lysis buffer was composed of 20 mL B-PER Bacterial Protein Extraction Reagent (Thermo Scientific, Waltham, MA), 150 mM NaCl, 2 mM B-ME, and one cOmplete EDTA-free protease inhibitor tablet (Roche Applied Science, Indianapolis, IN). The cell debris was removed by centrifugation, and the supernatant filter sterilized using a syringe capped with a pre-filter and a 0.45 µm pore filter. A purification column was prepared with 4 ml of HisPur Cobalt Resin (Thermo Scientific) washed once with sterile water and once with sterile 1X PBS. The filtered protein supernatant was applied to the column first, and was subsequently washed four times with 1X PBS + 10 mM imidazole and one wash with 1X PBS + 25 mM imidazole. Recombinant protein was eluted from the column with 1X PBS + 200 mM imidazole, and loaded into a 10K MWCO Slide-A-lyzer Dialysis Cassette (Thermo Scientific) to be dialyzed overnight in 3 L of 0.1X PBS stirring at 4°C. The protein was removed from the dialysis cassette and 200 units of thrombin (MP Biochemicals, Solon, OH) added, and allowed to incubate rocking overnight at room temperature. The mixture was then poured over a prepared 3 ml HisPur Cobalt Resin column, retaining the flow thru, which was concentrated to a final volume of 0.5-1 ml by centrifugation in a Amicon 3K Ultracel centrifugal filter unit (Millipore, Billerica, MA) and stored at 4°C on ice until use. The location of the expressed SarA protein was monitored throughout the purification process running all fractions collected on a polyacrylamide gel as previously described, stained and visualized.

Electrophoretic mobility shift assay (EMSA). The biotinylated probes were generated using PCR with the icaProBTFwd and icaProBTRev-BioTEG (Integrated DNA Technologies, Coralville, IA) primers from either MN8 or MN8m gDNA. A 6.5% non-denaturing polyacrylamide gel (30% acrylamide/ 0.8% bisacrylamide, 1X TBE, 100 µl of 10% ammonium persulfate, and 10 µl TEMED for 15 ml total volume) was prepared. Approximately 0.2 µg of either biotinylated probe was added to 40 µl of binding buffer-2 (20 mM HEPES pH 7.9, 1 mM DTT, 0.1 mM EDTA, 50 mM KCl, 5% glycerol, and 200 µg/ml BSA) containing 0.5 µg non-specific competitor DNA poly d(I:C), and incubated on ice for 10 minutes. Recombinant SarA was added at varying concentrations, allowed to incubate on ice for 30 minutes, and run in the prepared gel at 150 V for 1 hour in 0.25X TBE running buffer. A nylon membrane (Ambion, Austin, TX) was pre-wetted in 0.25X TBE, and the gel contents electrophoretically transferred in the same buffer for 1 hour at 40 V. DNA was UV cross-linked to the membrane using a Stratagene Stratalinker (La Jolla, CA) auto-crosslink function. Bands were visualized using the Thermo Scientific Chemilumiscent Nucleic Acid Detection kit (Waltham, MA) according to manufacturer's directions, with one modification: Pierce High Sensitivity Streptavidin-HRP (Thermo Scientific, Waltham, MA) was used at 1:10,000 in place of the kit reagent. After application of the working solution for 3 minutes, the membrane was covered in plastic wrap, exposed to X-ray film and developed in an X-O-Mat.

In silico *prediction of curvature/bendability.* The nucleotide sequence surrounding the *S. aureus* MN8m 5 bp deletion in the *ica* promoter region, as well as the same intact

region from strain MN8 was submitted to the bend.it server; which calculated the bendability/curvature propensity plots, using the DNase I-based bendability parameters of Bruckner et al. (1995) and the consensus bendability scale (Gabrielian & Pongor, 1996).

Analysis of intrinsic DNA bending. PCR was used to amplify the selected *ica* promoter region with the icaProBend1-Xba and icaProBend2-Sal primers from either MN8 or MN8m gDNA with directional restriction sites on either end of the PCR product. After gel electrophoresis and purification by gel extraction, the PCR product was restriction digested with XbaI and SalI (New England Biolabs, Ipswich, MA) according to manufacturer's specification. The plasmid pBEND2 was also digested with XbaI and SalI, prior to ligation of the digested *ica* promoter fragment inserts into the vector. The plasmid construct was used to transform chemically competent *E. coli* CH3 blue cells (Bioline, Tauton, MA) with transformants being selected for on LB agar plates containing ampicillin. The plasmid construct was isolated using the previously outlined plasmid mini-prep procedure in large quantity, and the sequence fidelity of the gene insert confirmed by nucleotide sequencing. Individual aliquots of approximately 100 µg of both the MN8 and MN8m-derived pBEND-icaPro constructs were restriction digested with BglII, NheI, SpeI, EcoRV, SspI, or BamHI (New England Biolabs). A 15 x 15 cm 10% polyacrylamide gel was prepared (1X Tris-Cl/SDS pH 8.8, 30% acrylamide/ 0.8% biasacrylamide, 350 µl of 10% ammonium persulfate, and 35 µl TEMED for 45 ml total volume). 1X loading buffer (5X stock composed of 25% glycerol and 2.5X TBE) was added to each of the plasmid digests prior to loading the gel, which was run at 30 V for

48 hours at 4°C. The gel was soaked in 0.5 µg/ml ethidium bromide for 30 minutes at room temperature and then visualized under UV light. DNA size was determined by comparison against the Hyperladder II DNA molecular weight marker (Bioline, Taunton, MA)

CHAPTER 3

Investigating the molecular mechanism responsible for *icaADBC* hyper-transcription in *Staphylococcus aureus* strain MN8m

Introduction

Gene regulation can be modulated by means beyond the ability of the nucleotide sequence of DNA to encode proteins; the physical and structural characteristics of the DNA molecule itself may play an important role in influencing gene expression. There is ample evidence for the importance of DNA flexibility in the action of DNA-binding proteins altering the physical conformation of bound DNA, either to effect gene regulation through positive or negative control. Rigid DNA curvature reduces its bendability, and intrinsic curvature of the DNA results from certain nucleotide sequences. Tracts of A or T longer than 3 base pairs are considered to be major determinants of intrinsic curvature, and extended poly-A or poly-T tracts exhibit a particularly high degree of rigid curvature (Perez-Martin & de Lorenzo, 1997). Therefore, mutations can impact cellular processes not only because of how the change to the specific sequence affects transcription/translation/protein function directly, but also in how they alter the physical DNA architecture of the region they occupy.

SarA is a major staphylococcal global regulator protein that has been implicated in the control of more than 120 different genes, and is an important positive regulator of

icaADBC transcription (Tormo *et al.*, 2005). SarA is a dimeric protein composed of a central helical core and two winged helix motifs that each contain a helix-turn-helix motif, and both of which are capable of binding DNA (Liu *et al.*, 2006). The winged domain recognizes the minor groove of DNA, while the helix-turn-helix interacts with the major groove. This binding of DNA compresses it, narrowing the minor groove and overwinding the helices, causing SarA-bound DNA to more closely resemble D-DNA that the more common B-DNA conformation (Schumacher *et al.*, 2001). Recent work has begun to expand our knowledge of SarA beyond the traditional role of a classical transcription factor. It is unique in that it appears to demonstrate highly promiscuous binding affinity (DNA, RNA, etc), and is present in much higher amounts at all stages of growth than classic transcription factors, but is not always functionally active (Fujimoto *et al.*, 2009). There is currently significant debate over how exactly SarA recognizes DNA, since binding is promiscuous and evidence of a consensus binding sequence thus far is weak and limited to AT-rich regions. An alternative theory was put forth by Fujimoto *et al*. (Fujimoto *et al.*, 2000) which suggests that SarA is an architectural protein that instead recognizes specific physical/topological characteristics of DNA for binding.

We have previously identified a spontaneous 5-bp deletion in the intergenic region between *icaA* and *icaR* that causes constitutive activation of the *icaADBC* operon, leading to an increase in PNAG production of up to 10,000-fold. The strain carrying this mutation, MN8m, has a distinct mucoid phenotype. However, the exact mechanism by which his small change induces such a profound increase in PNAG production remains unknown. We hypothesize that the deletion in the *icaADBC*

promoter region causes a significant change in the regional physical characteristics of the DNA, possibly allowing it to be more flexible in its interactions, leading to optimal transcriptional activation of *icaADBC.* We chose to include the interaction of SarA with our promoter region as a tool to better elucidate the mechanism responsible for increased PNAG production because it is a positive regulator of *icaADBC* that may influence transcriptional activity by altering the DNA topology/architecture. It is thought that it binds to and bends DNA in the 5' region of the gene in such a way as to alter the spacing between the -10 and -35 regions (Fujimoto *et al.*, 2009). We theorized that SarA binds to the *icaADBC* promoter region and maximizes the spacing, and that the 5-bp deletion responsible for the mucoid phenotype maximizes this spacing even in the absence of SarA.

Results

Effect of MN8m promoter deletion on intrinsic DNA curvature/flexibility

We have hypothesized that a potential molecular mechanism underlying the constitutive *icaADBC* transcription of strain MN8m may be related to the 5-bp deletion in its promoter region causing a significant change in the physical characteristic in that region of DNA. Preliminary *in silico* analysis was performed using the bend.it server (Vlahovicek *et al.*, 2003) to predict the effect of the deletion on the intrinsic DNA curvature and bendability of the 150 base pairs surrounding it (Fig. 4) since regions of bent DNA tend to span only a few dozen nucleotides. We found that alteration in the predicted characteristics was only observed in the 20 base pairs immediately

surrounding the deletion mutation site, a very small difference. We observed that the loss of those 5 base pairs reduced the predicted curvature of that region of DNA from approximately 3.0 °/helical turn to 0.5 °/helical turn, and slightly increased predicted bendability from 3.25 to 4 a.u. However, in general, values below 5.0 °/helical turn indicate a region of straight DNA with little to no curvature.

This observation was supported by our analysis directly comparing the intrinsic curvature of the altered DNA sequence *in vitro* using the plasmid vector pBEND2. The region of DNA from the *ica* promoter of both strains MN8 and MN8m inserted into the pBEND2 vector is shown in Figure 5.A. Use of the pBEND vector to determine curvature relies on the observation that the mobility of a DNA fragment in a polyacrylamide gel decreases as the center of any bent regions approaches the center of the fragment (Kim *et al.*, 1989). Therefore restriction digest of pBEND2 containing the *ica* promoter region yields fragments of identical size with location of the inserted DNA fragment being varied (Fig. 5.B). Electrophoresis of the digested inserts, which differ only in the position of the predicted bending center, was analyzed to determine K values from the ratio of observed size to actual size of the two inserts with the greatest observed difference (Fig. 6, Table 3). Supporting the assumption that predicted curvature values of less than 5.0 °/helical turn indicating a region of straight DNA, K values of approximately 1.1 indicate no significant point of bending. Additionally, these results determine that the 5-bp deletion responsible for the constitutive transcription of *icaADBC* in MN8m does not have a detectable effect on this aspect of DNA topology in its vicinity.

Figure 4. *In silico* prediction of bendability/curvature effects of the MN8m promoter deletion. Bendability/curvature propensity plots generated by the bend.it server for the nucleotide sequence 150 bp around the deletion site; the deletion site is outlined.

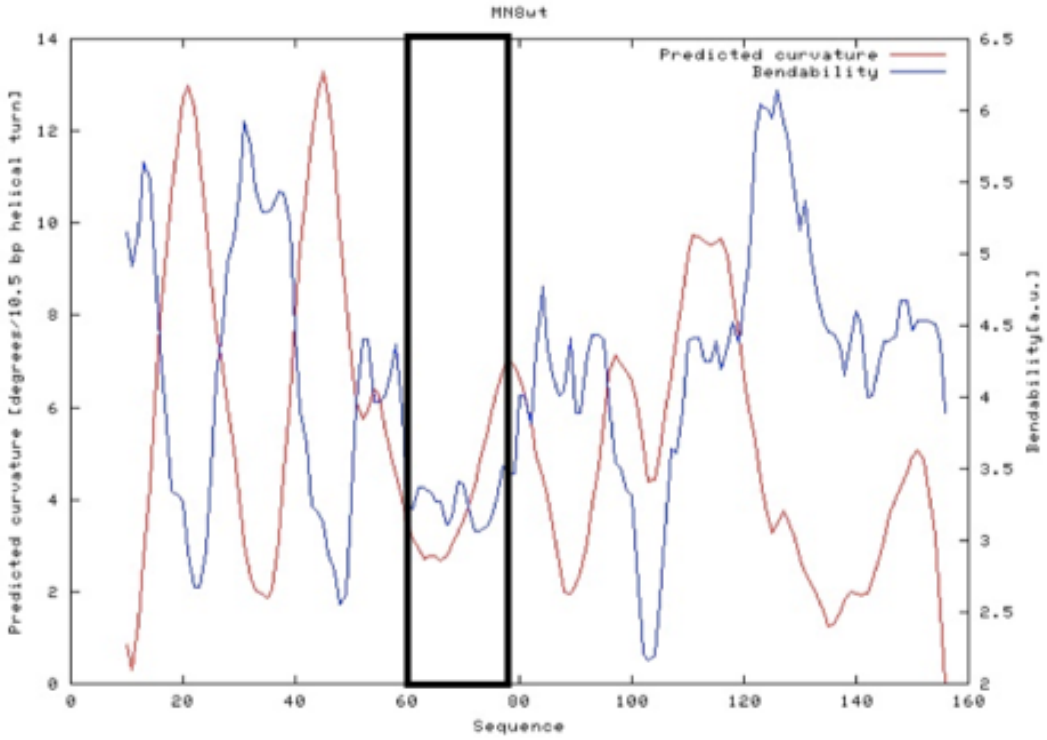

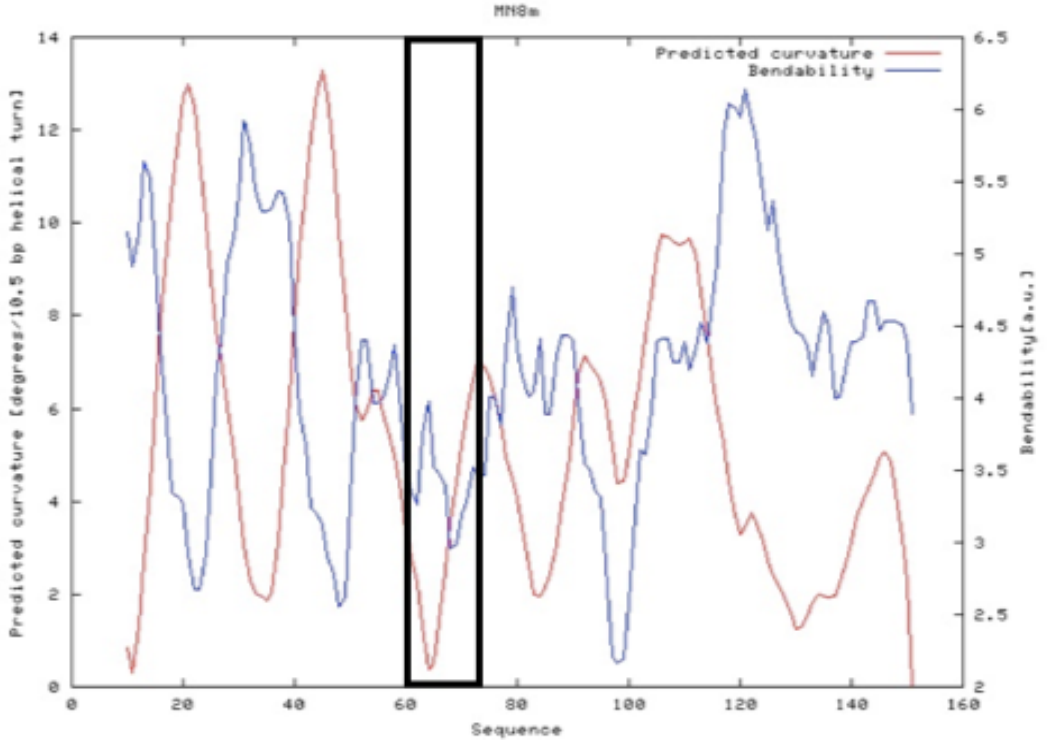

Figure 5: Schematic representation of the DNA sequence region to be inserted into the pBEND2 vector. A.) The region of DNA containing the MN8m deletion site to be inserted into the pBEND2 vector is highlighted in pink. Putative SarA binding sites are indicated by the red lines, and other promoter function sites are labeled. B.) The multiple cloning site of pBEND2 with reciprocal restriction digest sites. The fragments generated by BglII, NheI, SpeI, EcoRV, SspI, and BamHI restriction digest are shown with the position of the insert indicated.

A.

B.

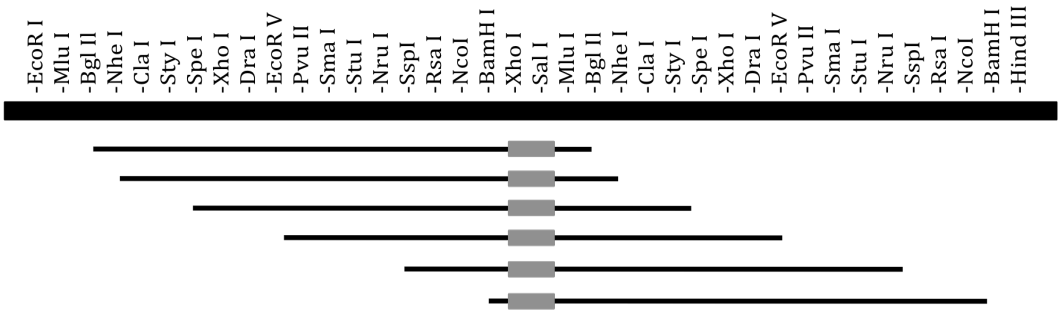

Figure 6: Analysis of intrinsic curvature of the promoter regions of *S. aureus* strains MN8 and MN8m. Restriction digests of pBEND2 containing either the MN8 or MN8m *ica* promoter segment electrophoresed on a polyacrylamide gel at 4°C, and visualized with ethidium bromide. Lane 1 contains BglII digested vector construct, lane 2 NheI, lane 3 SpeI, lane 4 EcoRV, lane 5 SspI, and lane 6 BamHI. The digested fragments selected for curvature analysis are indicated in the boxed areas.

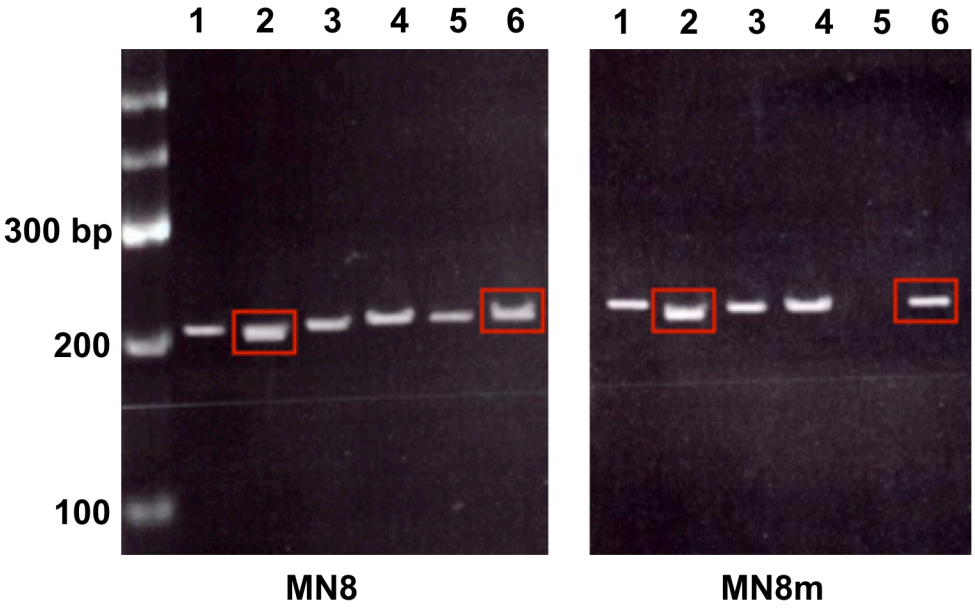

Table 3. Determination of MN8m *ica* promoter deletion on intrinsic DNA curvature

Strain Origin of Insert	Actual Size (bp)	Observed Size (bp)	K Value
MN8	203	215 - 230	1.059 - 1.133
MN8m	198	215 - 225	1.086 - 1.136

Expression and purification of recombinant SarA

The *S. aureus* global regulator SarA is an important positive regulator of *ica* that has been shown to bind in and around its promoter region (Tormo *et al.*, 2005). We speculated that the 5-bp promoter deletion in the strain MN8m might influence binding of SarA leading to the increased *icaADBC* expression. To investigate how SarA interacts with the intact versus deletion-modified promoter region, we first needed to heterologously express and purify recombinant SarA. The *sarA* gene was cloned into the IPTG-inducible pET32xT vector (generously supplied by Dr. David Williams, VCU, Richmond, VA), which attaches a C-terminal Thio-HIS tag to the protein. The recombinant protein was expressed in *E. coli* BL21-CodonPlus(DE3)-RIL cells. Expression of the expected Thio-HIS-tagged SarA product was confirmed by SDS-PAGE with the presence of a protein of approximately 34 kDa upon induction with 1 mM IPTG (Fig. 7.A), and by Western blot probed with 6X-HIS antisera showing a product of the same size after induction (Fig. 7.B). The expressed recombinant protein was isolated by column purification using cobalt resin (Fig. 8.A), and the Thio-HIS tag was removed by thrombin cleavage and separated from the 14.7 kDa SarA through repetition of cobalt column purification (Fig. 8.B).

SarA binding to the *ica* promoter region

To investigate our hypothesis that the MN8m deletion alters SarA binding to the *ica* promoter region, modulating PNAG expression, we utilized our purified recombinant SarA and the 100-bp region around the MN8m deletion (Fig. 9.A) for DNA binding gel shift assays. The DNA fragments from both MN8 and MN8m were

biotinylated and incubated with various amounts of the SarA protein, ranging from 0.01-0.9 µg, in the presence of the non-specific oligo competitor poly d(I:C). The EMSAs for both promoter fragments showed that the 5-bp deletion in strain MN8m had no discernable effect on SarA binding to that region (Fig. 9.B). The retarded protein-DNA complexes were visible for both strains beginning at 0.1 µg of SarA. A complete shift was observed between 0.05 µg and 0.1 µg of SarA (the lower band for MN8 at 0.2 µg SarA was not observed in independent replicates, and variance in band intensity is experimental artifact). These results indicated that partial binding could be observed at SarA amounts between these two concentrations to further characterize the DNA-binding affinity of SarA to this sequence fragment. Additionally, shifted bands of different sizes were observed at SarA amounts greater than 0.3 µg, supporting the existence of several SarA-binding sites within this region of the *icaADBC* promoter.

Effect of SarA on the mucoid phenotype of MN8m

While we observed that the 5-bp deletion in the *icaADBC* promoter responsible for the mucoid phenotype of *S. aureus* strain MN8m does not affect SarA binding affinity for the region, we wanted to further elucidate the potential role of this positive regulator on the hyper-activation of the operon. It is thought that SarA binds to and bends promoter DNA in such a way as to optimize spacing, generally between the -10 and -35 regions, and promote transcription (Fujimoto *et al.*, 2009). We theorized that SarA binds to the *icaADBC* promoter region and maximizes the spacing (although it does not lie between the -10 and -35 regions) and that the 5-bp deletion responsible for the mucoid phenotype maximizes this spacing even in the absence of SarA. To investigate this

Figure 7: Heterologous expression of *S. aureus* 6X-HIS-tagged recombinant SarA in *E. coli*. (A) Imperial-stained SDS-PAGE of cell lysates of uninduced *E. coli* BL21-CodonPlus(DE3)-RIL containing pET32xT-*sarA,* and the same strain induced for 2 hours with 1 mM IPTG. Approximate molecular weights indicated. (B) Western blot of the same cell lysates probed with anti-6X-HIS Tag antiserum. Approximate molecular weights indicated.

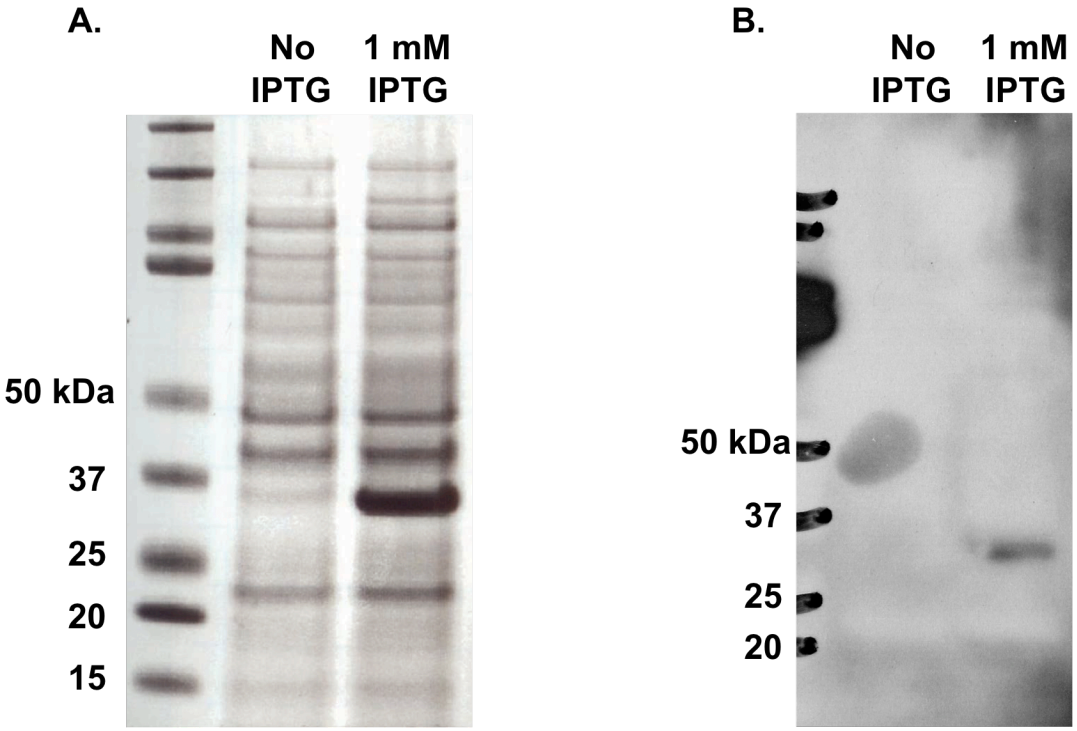

Figure 8: Purification of *S. aureus* recombinant SarA. (A) Purification of 6X-HIS tagged recombinant SarA from culture lysate of IPTG-induced *E. coli* BL21-CodonPlus(DE3)-RIL containing pET32xT-*sarA* using a cobalt resin column. An Imperial-stained SDS-PAGE gel, in which Lane 1 contains initial flow through after application of the culture lysate, Lane 2 represents the beginning of four column washes with 1X PBS + 10mM imidazole, Lane 3 contains a single wash with 1X PBS + 25mM imidazole, Lane 4 elution of the bound protein with 1X PBS + 200mM imidazole, and Lane 5 contains the remaining cobalt resin. Approximate molecular weights are indicated. (B) An Imperial-stained SDS-PAGE gel of the previous protein elution after treatment with thrombin to cleave the Thio-HIS tag from the recombinant SarA, and passage over a cobalt column to remove the tag. Approximate molecular weights are indicated.

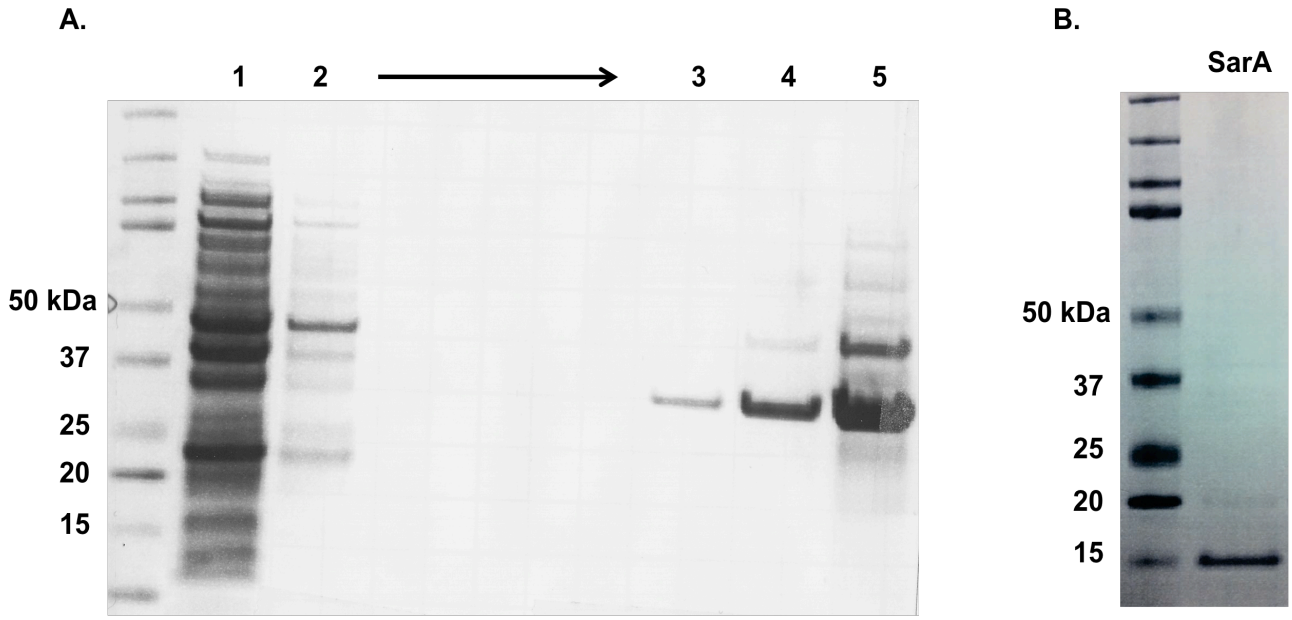

Figure 9: Comparison of SarA binding to the MN8 and MN8m *ica* operon promoter regions. (A) Schematic representation of the nucleotide sequence (highlighted in pink) from both MN8 and MN8m that was biotinylated for use as specific binding probes. Putative SarA binding sites are indicated by red lines. (B) Electrophoretic mobility shift assays with biotinylated specific probes and non-specific competitor DNA, used to detect binding of SarA to the selected region of *S. aureus* strains MN8 and MN8m. Membranes were x-ray visualized after electrophoresis and electrophoretic transfer with streptavidin-HRP.

A.

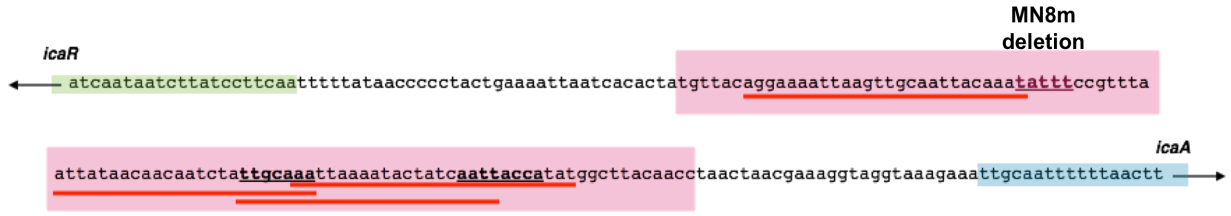

B.

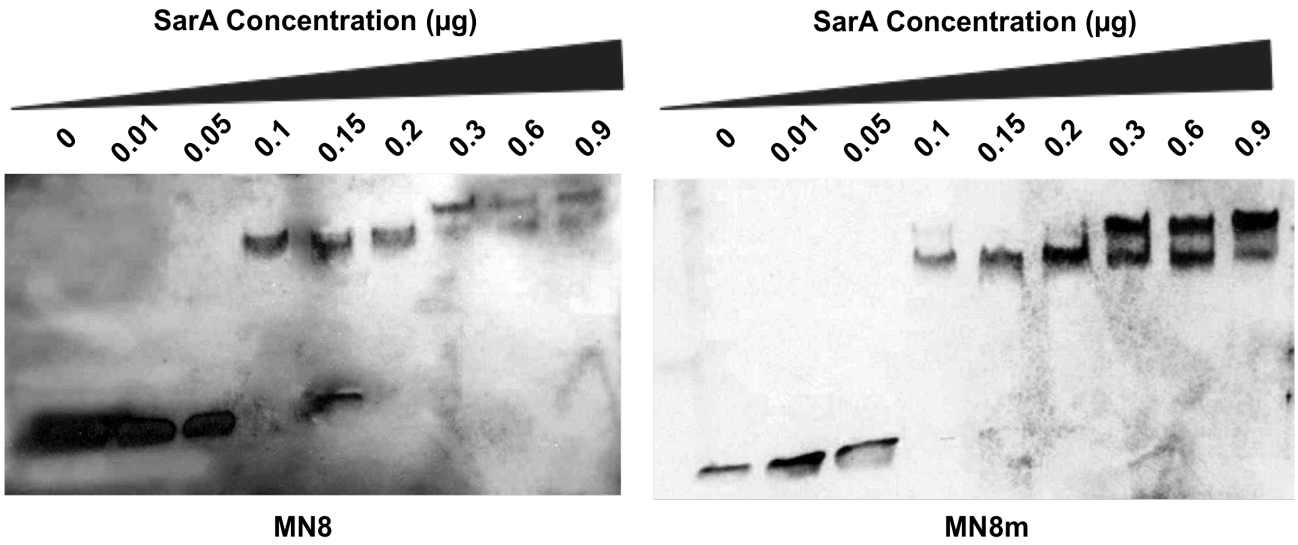

hypothesis that SarA is non-essential for *icaADBC* expression in MN8m, we first constructed a group of isogenic *S. aureus* mutant strains: RN4220Δ*ica*, RN4220Δ*ica*+pBT9-M1 (in which the deletion has been complemented *in trans* by the entire *icaRADBC* locus under the control of the MN8m-type promoter on the vector pBT9), and RN4220Δ*ica*Δ*sarA*+pBT9-M1. When these three strains were plated on Congo red agar (CRA), we observed only non-mucoid colonies as expected for the PNAG-negative strain RN4220Δ*ica*, which are slick, circular, and occasionally surrounded by a transparent red perimeter (Fig. 10). However, RN4220Δ*ica*+pBT9-M1 and its isogenic *sarA* mutant strain RN4220Δ*ica*Δ*sarA*+pBT9-M1 both formed mucoid colonies similar to those observed in strain MN8m, which appear dry with irregular edges.

The observation that there was no discernible difference in the mucoid colony morphology between the SarA-positive and SarA-negative strains, suggested that SarA may not be required for PNAG synthesis in strains containing the 5 bp deletion in the *icaADBC* promoter. To test this, we performed slot-blot analysis using PNAG-specific rabbit polyclonal antiserum. As depicted in Figure 11, no PNAG was detected in the *ica*-negative strain, while it was detected on the surface of both RN4220Δ*ica*+pBT9-M1 and RN4220Δ*ica*Δ*sarA*+pBT9-M1, supporting the previous observation of a mucoid phenotype. Not only was SarA not required for PNAG synthesis, but there actually appeared to be more PNAG present in the SarA-negative cultures, indicating a potential negative effect of SarA on expression of the mucoid *icaADBC* operon.

Role of SarA in MN8m *icaADBC* hyper-transcription

The *icaADBC* genes are co-transcribed, so to determine the influence of SarA on levels of the full-length transcript produced by the mucoid promoter, we quantified levels of the 3'-most transcript, *icaC*, by realtime RT-PCR. As shown in Figure 12, *icaADBC* transcript levels were more than 30-fold greater in RN4220Δ*ica*Δ*sarA*+pBT9-M1 than in the isogenic SarA-positive strain RN4220Δ*ica*+pBT9-M1. These results support the previous observation that SarA is not essential for *icaADBC* expression from the mucoid promoter. Furthermore, it appears that in the presence of the MN8m promoter deletion, SarA has a negative impact on transcriptional activation.

Discussion

Virtually nothing is known about the molecular mechanism underlying the constitutive production of PNAG in *S. aureus* strain MN8m, aside from the fact that it is caused by a 5 bp deletion in the *icaADBC* promoter region. We have hypothesized that the increased transcriptional activation of *icaADBC* may be due to the mutation altering the topology or physical traits of the DNA structure in its vicinity. We have predicted and confirmed that the DNA in the *icaADBC* promoter region is predominantly linear, with no detectable intrinsic curvature, and that this does not change when the MN8m deletion is present. However, while we have shown that there is no intrinsic bend in the *icaADBC* promoter, this does not rule out that the 5 bp deletion in MN8m could increase DNA-binding protein-induced curvature to better stimulate transcription or relieve repression. Additionally, one alternative theory that should be pursued further is that the 5 bp

Figure 10: Effect of *sarA* on mucoid colony morphology. Bacterial colonies from strains RN4220Δ*ica*, RN4220Δ*ica*+pBT9-M1, and RN4220Δ*ica*Δ*sarA*+pBT9-M1 were grown on Congo red agar (CRA). Strains containing pBT9 were grown on CRA containing chloramphenicol.

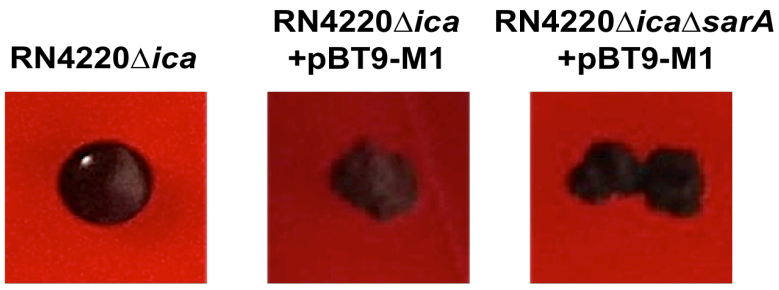

Figure 11: Effect of *sarA* on PNAG production. PNAG slot blot analysis of *S. aureus* strains producing different amounts of plasmid encoded PNAG; probed with PNAG-specific polyclonal antiserum. Samples for both strains containing the mucoid plasmid pBT9-M1 were diluted 1:10 further than indicated prior to immobilization on membrane.

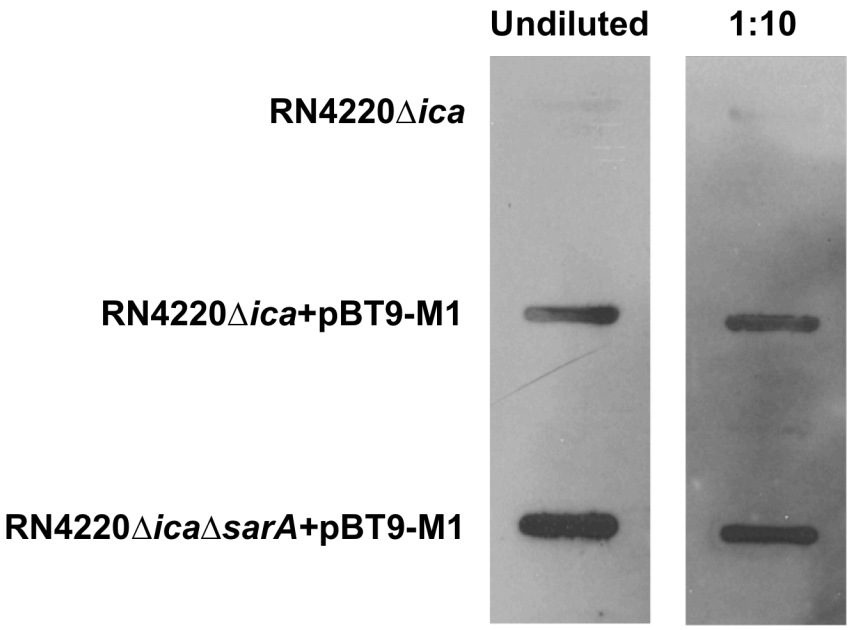

Figure 12: Effect of *sarA* on *ica* mRNA transcript levels. Real-time RT-PCR analysis of *icaC* mRNA transcript was performed. Bars represent the mean fold difference in transcript amount relative to strain RN4220Δ*ica*+pBT9-M1 with biological replicates n = 3, and error bars indicate the standard deviations. Statistical comparison (unpaired t test) of RN4220Δ*ica*+pBT9-M1 versus RN4220Δ*ica*Δ*sarA*+pBT9-M1 gave a P value of <0.0015.

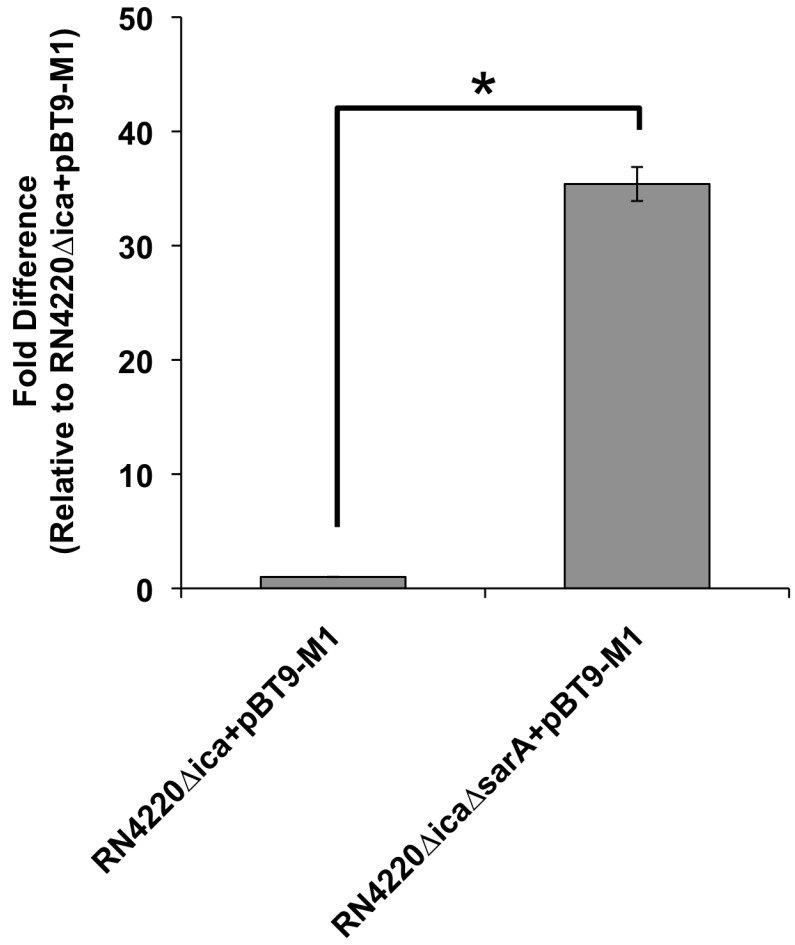

deletion produces its effect by inducing a 180 degree turn in the helical face of downstream DNA elements, potentially optimizing transcription activating interactions (between RNA polymerase and DNA, or another effect0r protein).

SarA is a positive regulator of icaADBC transcription that is known to bind to the *ica* promoter region (Tormo et al., 2005). While the exact binding site(s) is not known, we observed that the MN8m 5 bp deletion disrupts a putative SarA binding site as suggested by Tormo et al. (2005), leading us to hypothesize that binding of SarA might be altered in strain MN8m, increasing *icaADBC* transcription. However, we demonstrated through electrophoretic mobility shift assays that there is no detectable difference in the binding affinity of SarA to either the MN8 or MN8m promoter regions. We were able to conclude that there are likely to be multiple SarA binding sites within this region of DNA; and although it is not clear exactly where on the DNA SarA is binding, we intend to use our existing system to identify the preferred SarA binding sites to determine if sequence consensus is important. It is also worthy to note that we have devised a reliable *in vitro* method for heterologous expression and efficient purification of large quantities of recombinant SarA that is functionally active.

The most interesting observations of our work addressed the involvement of SarA in the constitutive transcriptional activation of *icaADBC* in MN8m. We initially theorized that while SarA is still capable of binding the promoter in such a way as to alter DNA element spacing (although it does not lie between the -10 and -35 regions), the 5-bp deletion responsible for the mucoid phenotype maximizes this spacing even in the absence of SarA, rendering SarA non-essential for *ica* expression in MN8m. This hypothesis has thus far been supported by our observations that the mucoid colony

morphology and hyper-PNAG production is maintained in a SarA-negative mucoid strain background. However, we concurrently observed that not only was SarA not necessary but that its absence increased *icaADBC* transcript levels and detectable PNAG production. These results expanded our hypothesis to include the likelihood that not only is SarA no longer responsible for *ica* expression, its presence appears to interfere with transcriptional activation. This conclusion is unique in that SarA is a well-characterized positive regulator of *icaADBC*, and here we have demonstrated that in the MN8m strain background it acts as a negative regulator. This is possibly due to the physical presence of SarA bound to the promoter sterically hindering even greater transcription initiation by another effector, possibly RNA polymerase alone (auto-activation of transcription) or other unknown transcription factors.

CHAPTER 4

Characterizing Novel Phase Variation of Poly-N-Acetylglucosamine in *Staphylococcus aureus*

Introduction

Phase variation functions as a reversible on/off switch for the expression of a particular gene. The result is commonly an alteration in the expression of some cell surface-expressed antigen. Slipped-strand mispairing is one mechanism that can lead to the production of a phase variant. Slipped-strand mispairing occurs during DNA replication when there is mispairing between mother and daughter DNA strands in regions of DNA that contain simple 1-10 nucleotide repeats (Levinson & Gutman, 1987). This results in the addition or subtraction of one or more repeats that can bring about a change in transcriptional efficiency or shift the reading frame to alter or halt translation.

We found previously that a 5-nucleotide deletion mutation within the *icaADBC* promoter of strain MN8m was sufficient to induce constitutive transcription of the *icaADBC* genes and high-level PNAG production, resulting in a mucoid phenotype and strong biofilm production (Jefferson et al., 2003). In the present study, we noted that growth of the mucoid strains in liquid culture resulted in the rapid accumulation of non-mucoid variants suggesting that either mutation to the non-mucoid phenotype occurred at high frequency or that the non-mucoid variants had a selective growth advantage. We

investigated this phenomenon and found that the most frequent mutation leading to the phenotypic variation was a slipped-strand mispairing in *icaC*.

Results

Non-mucoid variants accumulate in cultures of a mucoid *S. aureus* strain

S. aureus strain MN8m is a spontaneous PNAG-overproducing mutant of strain MN8 (Jefferson *et al.*, 2003). It is highly aggregative in liquid culture whereas non-mucoid strains are dispersed, making the culture turbid (Fig. 13). We found that MN8m cultures frequently exhibited an appearance that was somewhere between that of a turbid, non-mucoid strain and an auto-aggregative mucoid strain (Fig. 13). When these cultures were plated on Congo red agar (CRA), both mucoid colonies, which appear dry with irregular edges, and non-mucoid colonies, which are slick, circular, and occasionally surrounded by a transparent red perimeter, were observed (Fig. 14). Several of the non-mucoid MN8m variants were isolated and assigned names based on JB10-22; one of the strains selected for further characterization was JB12. We compared the biofilm-forming ability of the non-mucoid variant JB12 to MN8 (the strain from which MN8m derived), which produces a low level of PNAG (considered wild-type), and to the PNAG-negative strain MN8*Δica* (Fig. 15). The JB12 strain displayed a significant decrease in biofilm formation, most closely resembling the PNAG-negative strain MN8*Δica*.

Analysis of non-mucoid variant JB12 to determine PNAG expression

The finding that JB12 biofilms resembled those of the PNAG-negative strain

Figure 13: Variation in MN8m planktonic growth phenotype. Liquid cultures in TSBG of (A) highly aggregative mucoid MN8m, (B) non-mucoid MN8, and (C) MN8m with mixed appearance.

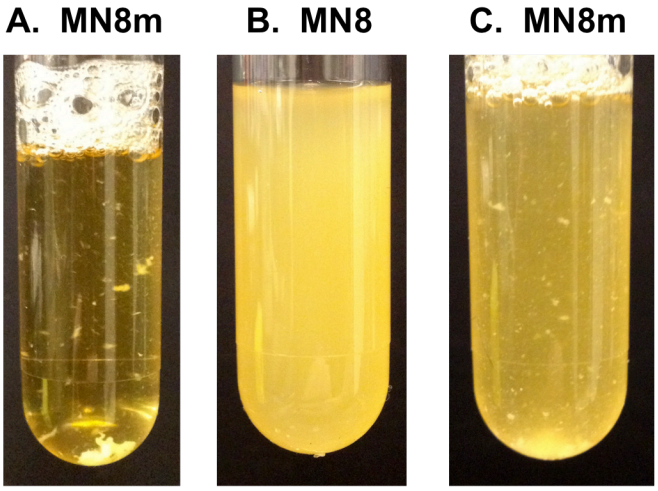

Figure 14. Colony morphology of non-mucoid variants isolated from mucoid strain MN8m. Bacterial colonies of MN8, MN8Δ*ica,* MN8m, and the JB12 and JB17 variants on Congo red agar (CRA) plates.

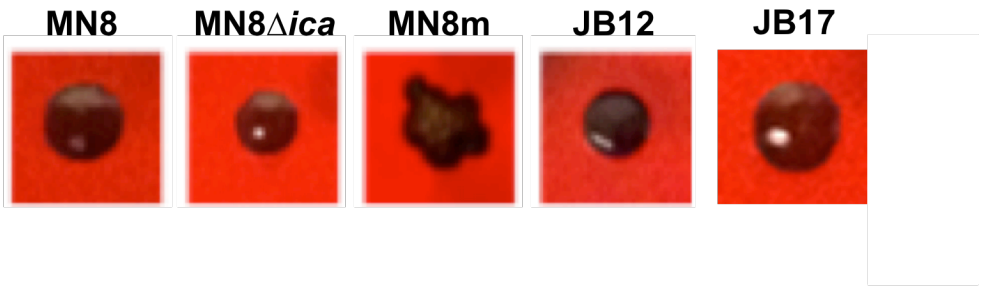

Figure 15. Biofilm formation by the non-mucoid variant, JB12. Biofilm formation was assessed by visualization of biofilms formed on microtiter plate wells by safranin staining and quantitative data was obtained by resuspending the safranin in acetic acid. Bars represent the mean $OD_{562\ nm}$ of n = 6, and error bars indicate the standard deviations. Statistical comparison (unpaired t test) of MN8m versus JB17 gave a P value of <0.001.

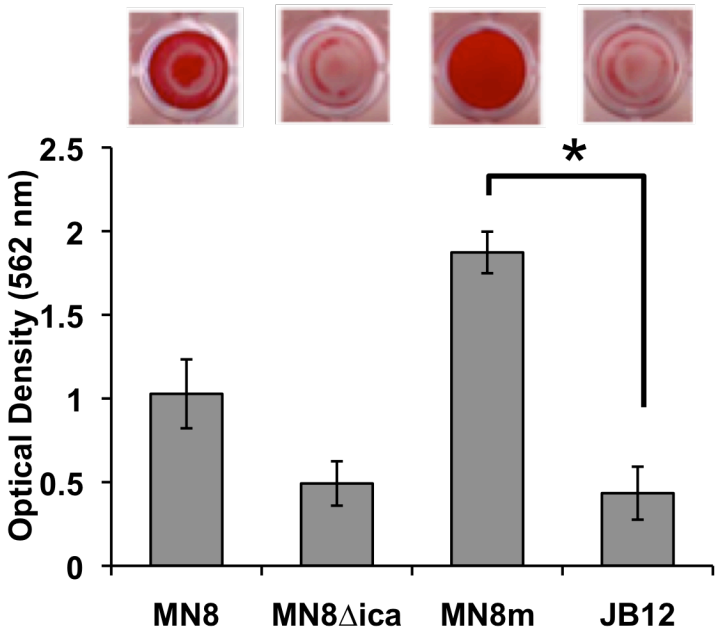

MN8Δ*ica* suggested that PNAG production was severely abrogated or absent in JB12. To test this, we performed slot-blot analysis using PNAG-specific rabbit polyclonal antiserum. As depicted in Figure 16, no PNAG was detected on the cell surface or in the spent media of JB12 cultures. Therefore, the molecular mechanism leading to the non-mucoid phenotype appeared to be mediating the variation through the loss of detectable levels of PNAG.

icaADBC transcript level of JB12

A 5 bp deletion in the *icaADBC* promoter region of MN8m is responsible for constitutive *icaADBC* transcription and the constitutive hyper-production of PNAG that characterizes strain MN8m (Jefferson et al., 2003). We sequenced this region of DNA in strain JB12 and found that the *ica* promoter region was identical to MN8m. The *icaADBC* genes are co-transcribed, so to determine levels of the full-length transcript, we quantified levels of the 3'-most transcript, *icaC*, by realtime RT-PCR. As shown in Figure 17, *icaADBC* transcript levels were more than 300-fold greater in MN8m than in the non-mucoid parent strain MN8 and the level remained elevated in the non-mucoid variant. These results indicate that the loss of PNAG production was not due to a decrease in the level of *icaADBC* transcript, but rather that it was mediated by a post-transcriptional mechanism affecting PNAG synthesis.

Identification of a frequent mutation within a repeat region of *icaC*

Since the 5 bp promoter deletion remained and there was no detectable

Figure 16. PNAG production by the non-mucoid variant, JB12. PNAG slot blot analysis of *S. aureus* strains producing different amounts of PNAG; probed with PNAG-specific polyclonal antiserum. Samples for both MN8m cell surface and spent media were diluted 1:10 prior to immobilization on membrane.

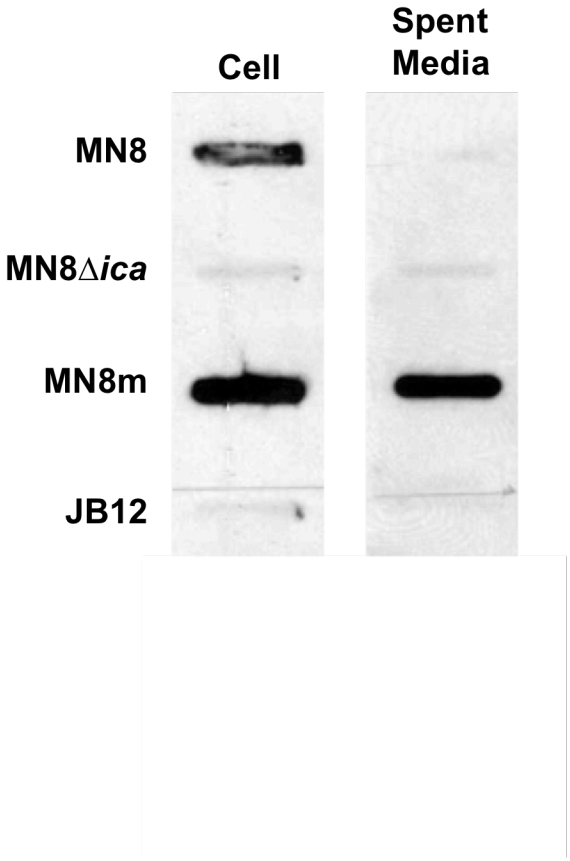

Figure 17. Levels of *ica* transcript in the non-mucoid variant, JB12. Real-time RT-PCR analysis of *icaC* mRNA transcript was performed. Bars represent the mean fold difference in transcript amount relative to strain MN8 with n = 3, and error bars indicate the standard deviations. Statistical comparison (unpaired t test) of MN8m and JB12 versus MN8 gave a P value of <0.001.

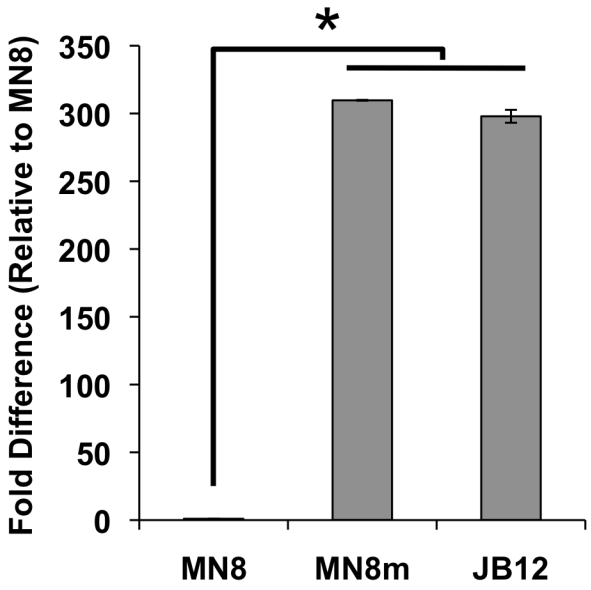

difference in i*caADBC* transcript levels, DNA sequencing of the entire operon was performed. A 4 bp insertion was identified in the coding region of *icaC* (Fig. 18), extending a small region of "ttta" repeats from three units to four. The insertion led to a shift in the translational reading frame and truncation of the protein, reducing IcaC from 350 amino acids to 303.

To confirm that the nucleotide insertion was responsible for loss of the mucoid phenotype, we complemented the *icaC* gene in trans. Expression of the intact *icaC* gene in strain JB12 from the IPTG-inducible plasmid pCL15, lead to restoration of the mucoid colony morphology on CRA plates (Fig. 19), PNAG synthesis (Fig. 21), and biofilm formation (Fig. 20). Introduction of the empty vector into the variant had no effect.

Additionally, we found that variations in the number of 4 bp repeats in this region appears to be a frequent mutation among non-mucoid variants isolated from pure MN8m cultures. The *icaADBC* loci of twelve isolates with the PNAG-negative phenotype from different cultures were sequenced. Seven of these were shown to have either insertion or deletion of a repeat unit in the same region. Furthermore, examination of published *S. aureus* sequences revealed three clinical MRSA strains (TW20, JKD6008, and T0141) and two partially sequenced clinical isolates (SA21178 and SA21342) exhibiting 2-3 additional repeat units (Fig. 22) demonstrating that the phase variants occur *in vivo*.

Figure 18. Schematic representation of the *ica* locus showing the position of the 4 bp insertion in the region of repeats identified in *icaC* of the non-mucoid variant JB12.

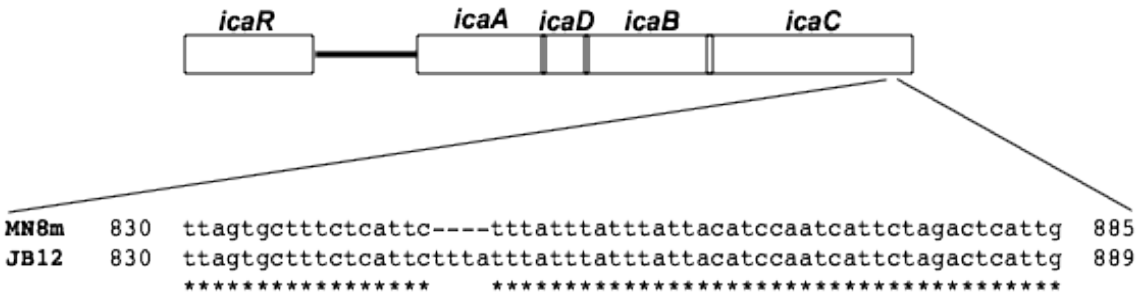

Figure 19. Effect of complementation of JB12 with *icaC in trans* on colony morphology. Bacterial colonies of MN8 and JB12 and JB12 on Congo red agar (CRA), and JB12+empty vector or *icaC* on CRA+Cm+ 1mM IPTG.

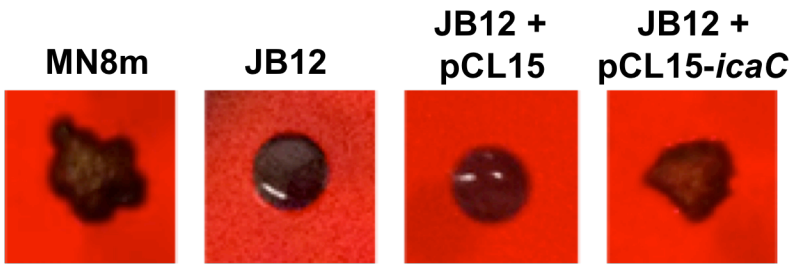

Figure 20. Effect of complementation of JB12 with *icaC in trans* on biofilm formation. Biofilms formed in TSBG or TSBG+Cm+1mM IPTG on microtiter plate wells were stained with safranin and the safranin was quantified by resuspending in acetic acid and measuring OD562 nm. Bars represent the mean of 6 replicates, and error bars indicate the standard deviations. Statistical comparison (unpaired t test) of JB12+pCL15 (empty vector) versus JB12+pCL15-*icaC* gave a P value of <0.001.

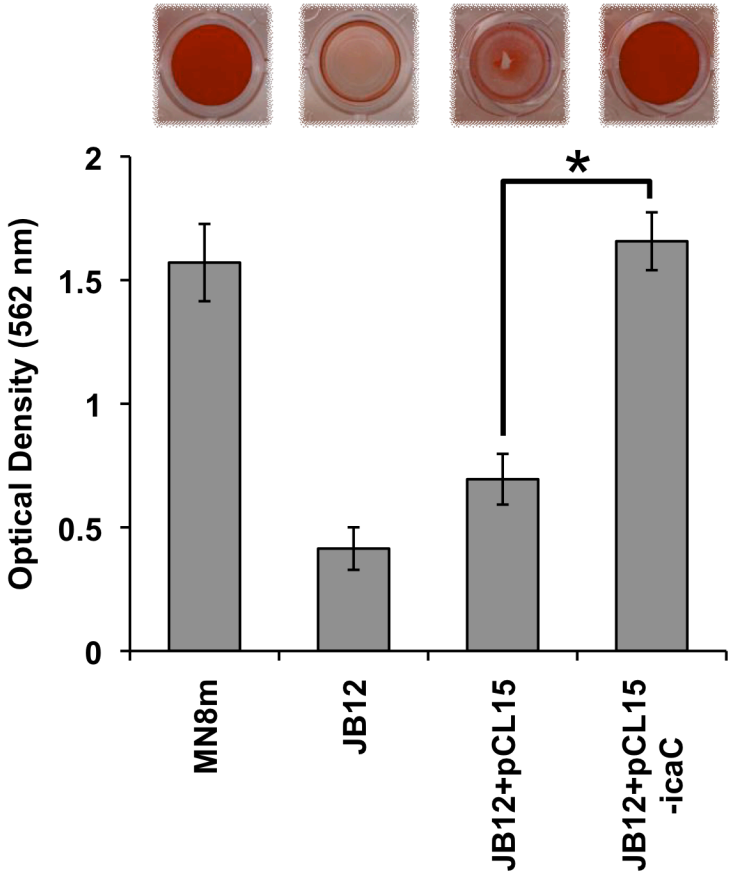

Figure 21. Effect of complementation of JB12 with *icaC in trans* on PNAG production. PNAG slot blot of cell surface fractions cultured in TSBG or TSBG+Cm+1mM IPTG probed with polyclonal anti-PNAG antiserum (MN8m and JB12+pCL15-*icaC* samples were diluted 1:10 prior to immobilization on membrane whereas JB12 and JB12+pCL15 were not diluted).

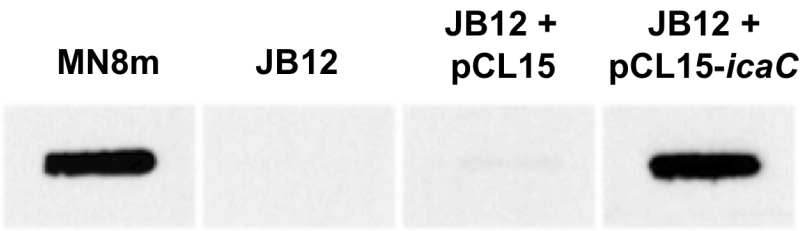

Figure 22. Nucleotide sequence alignment of the region of repeats identified in i*caC*. Comparison of mucoid MN8m and non-mucoid isolate JB12 with five published sequences of *S. aureus* clinical isolates.

```
MN8m       781   ggtatttgcacgcattttaaaacaatgttatttaatacgattcaaatgattagtgctttc   840
JB12             ggtatttgcacgcattttaaaacaatgttatttaatacgattcaaatgattagtgctttc
21342            ggtatttgcacgcattttaaaacaatgttatttaatacgattcaaatgattagtgctttc
TW20             ggtatttgcacgcattttaaaacaatgttatttaatacgattcaaatgattagtgctttc
21178            ggtatttgcacgcattttaaaacaatgttatttaatacgattcaaatgattagtgctttc
JKD6008          ggtatttgcacgcattttaaaacaatgttatttaatacgattcaaatgattagtgctttc
T0131            ggtatttgcacgcattttaaaacaatgttatttaatacgattcaaatgattagtgctttc
                 ************************************************************

MN8m       841   tcattc------------tttatttatttattacatccaatcattctagactcattgttt   888
JB12             tcattc--------tttatttatttatttattacatccaatcattctagactcattgttt
21342            tcattc--------tttatttatttatttattacatccaatcattctagactcattgttt
TW20             tcattc----tttatttatttatttatttattacatccaatcattctagactcattgttt
21178            tcattc----tttatttatttatttatttattacatccaatcattctagactcattgttt
JKD6008          tcattctttatttatttatttatttatttattacatccaatcattctagactcattgttt
T0131            tcattctttatttatttatttatttatttattacatccaatcattctagactcattgttt
                 ******            ******************************************

MN8m       889   gcatatacaaatatatttgaggataatacaatggtctttctagcgatatcactactattc   948
JB12             gcatatacaaatatatttgaggataatacaatggtctttctagcgatatcactactattc
21342            gcatatacaaatatatttgaggataatacaatggtctttctagcgatatcactactattc
TW20             gcatatacaaatatatttgaggataatacaatggtctttctagcgatatcactactattc
21178            gcatatacaaatatatttgaggataatacaatggtctttctagcgatatcactactattc
JKD6008          gcatatacaaatatatttgaggataatacaatggtctttctagcgatatcactactattc
T0131            gcatatacaaatatatttgaggataatacaatggtctttctagcgatatcactactattc
                 ************************************************************
```

Isolation of JB12 mucoid variants

Phase variation is, by definition, an on/off switch. Therefore, if the mutation that we isolated was a product of phase variation, then we would expect the variant JB12 to revert to the mucoid phenotype. To determine whether or not the phenotype was reversible we plated cultures of JB12 onto CRA. We did not observe any mucoid colonies initially when we plated JB12, so we grew cultures on tissue culture-treated polystyrene for 36 hr to encourage adherence of PNAG-producing bacteria and plated the adherent fraction onto CRA. This selection method resulted in the isolation of mucoid colonies. To confirm that these JB12 mucoid variants supported our theory of phase variation and did not have a compensatory mutation elsewhere it the genome of *ica* locus, we sequenced 6 isolates from separate cultures. All 6 variants sequenced had lost the 4 bp repeat unit that was gained in JB12 meaning that they had reverted to MN8m genotype. These results support a mechanism of phase variation through slip-strand mispairing. However, the requirement for a selection process to isolate mucoid revertants suggested that the number of revertants was very low. We hypothesized that this was due to a fitness cost imparted by high-level PNAG production.

Fitness cost of PNAG over-production

To determine if there was a fitness cost associated with constitutive PNAG synthesis, we inoculated competitive co-cultures of MN8m and JB12 equally and examined shifts in the population over time by assessing colony morphology on CRA. We observed that there does indeed appear to be significant growth advantage in the PNAG-negative variant JB12. Growth curves revealed slower growth in MN8m relative to JB12 (Fig. 23), while competitive co-culture of equal amounts MN8m and JB12

showed that JB12 almost completely took-over the culture in a relatively short amount of time (Fig. 24). Direct calculation of the fitness cost of PNAG over-production versus PNAG loss resulted in fit_t (relative bacterial fitness) values of +1.401 at 6 hours, and +1.386 at 12 hours, with a value greater than 1 indicating a significant fitness advantage of the JB12 PNAG-negative phenotype over the mucoid MN8m.

Effect of partial function of PNAG synthesis pathway on cell survival

Since only the function of IcaC appears to be altered in this phase variable control of PNAG production, we hypothesized that the remaining components of the synthesis pathway (IcaA, IcaD, and IcaB) that are still present in functional forms may have alternative roles within the cell. We compared the growth rates in liquid culture of MN8Δ*ica*, which lacks all four genes and produces no PNAG synthesis proteins, and JB12, which has intact IcaA, IcaD, and IcaB, but found no difference. However, under starvation conditions, when the strains were switched to incubation in minimal media containing no carbon source, there was a significant difference in bacterial survival (Fig. 25). Production of intact, and presumably functional IcaA, IcaD, and IcaB significantly increased survival of JB12 under these growth-limiting conditions.

Discussion

This study was based upon our observation that cultures of the mucoid strain MN8m frequently appeared to be a mixture of mucoid and non-mucoid bacteria. We hypothesized that either there was a molecular mechanism for phase variation resulting in a mutation frequency higher than what would be expected for random mutagenesis or

Figure 23. Growth comparison of MN8m and JB12. Strains were grown in TSBG. Points represent the mean percent value of $OD_{600\ nm}$ at each time point with n = 3, and error bars indicate the standard deviations.

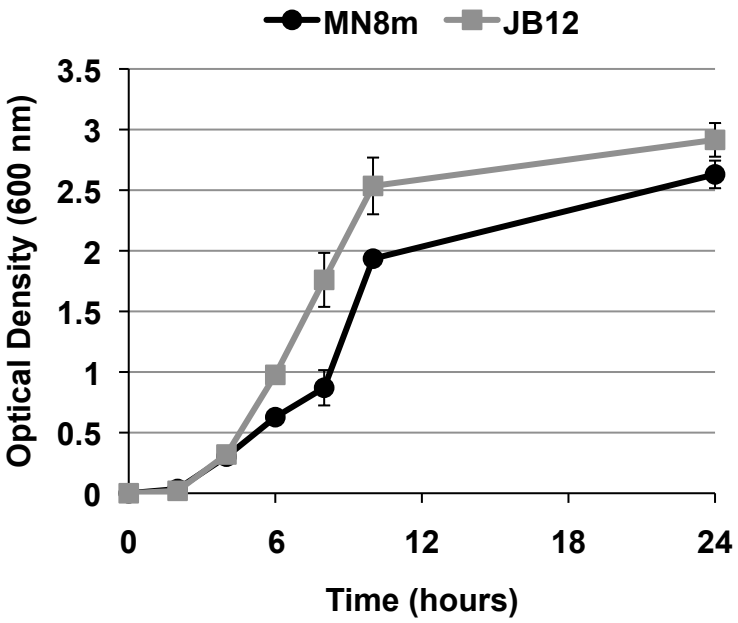

Figure 24. Fitness of MN8m versus JB12. The competitive fitness of MN8m in co-culture with PNAG-negative, non-mucoid JB12 was determined by combining the two strains and enumerating each strain over time. Bars represent the value of each phenotype as a percent of total population, determined by enumerating colonies on CRA. Values represent the mean of triplicate samples.

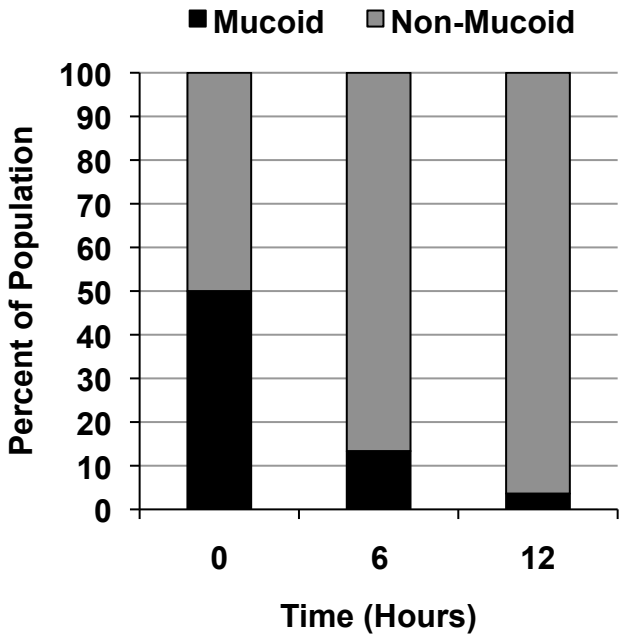

Figure 25. Influence of partial function in PNAG synthesis pathway on survival in minimal media. MN8m and JB12 were initially grown overnight in TSBG. The cells were collected and resuspended in minimal media lacking a carbon source to mimic starvation conditions. Points represent the mean percent value of cells enumerated at each time point relative to the starting populations with n = 3, and error bars indicate the standard deviations. Statistical comparison (unpaired t test) of MN8Δ*ica* and JB12 at 10 hours and 24 hours gave a P value of <0.001.

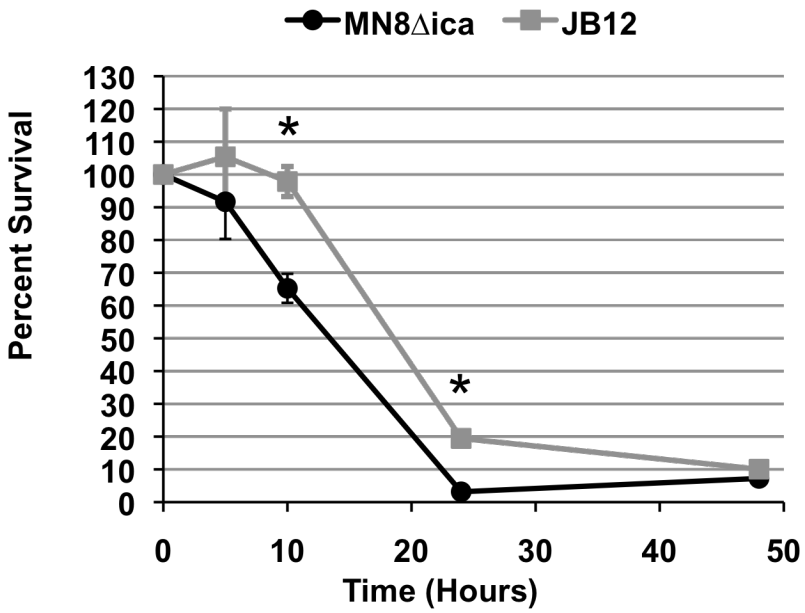

that overproduction of PNAG was detrimental to growth and was associated with a strong selection bias for mutants. We attempted to determine the mutation frequency; however, results from different biologic replicates varied by over four orders of magnitude. We found that there was a strong competitive advantage for the non-mucoid variants. The growth advantage is likely responsible for the wide variation in apparent mutation frequency. Depending on the time-point during culture at which a mutation leading to the non-mucoid phenotype occurred, the variants would have more or less time to increase in numbers relative to the parent strain due to the growth advantage. Therefore, the final number of variants present at the end of the culture period would depend upon the timing of the first mutation event and would be stochastic.

The growth advantage of the non-mucoid variants also explains our difficulty in isolating mucoid revertants from non-mucoid cultures. We had to grow cultures on tissue culture-treated polystyrene for three days and select for adherent bacteria in order to detect mucoid revertants on CRA. Due to the fitness cost associated with PNAG hyper-production, numbers of mucoid revertants would remain very low relative to the non-mucoid parent population.

Despite our finding that the PNAG-negative variants enjoyed a fitness advantage, we hypothesize that it is unlikely for PNAG-negative variants to have a fitness advantage *in vivo*. Firstly, we were working with a mucoid variant that arose *in vitro* and produces approximately 1,000-fold more PNAG than most clinical isolates. Constitutive hyper-production of this large polysaccharide almost certainly bears a high metabolic cost, whereas normal, low-level PNAG production would not. Secondly, *in vivo*, PNAG

plays an important role in immune evasion and PNAG-negative variants would likely be more susceptible to neutrophil-mediated killing. It appears that antibody-mediated immunity against PNAG is somewhat complex and that only antibodies against deacetylated PNAG effectively mediate opsonophagocytosis (Maira-Litran et al., 2005). However, in the event that the host mounts an effective immune response, the capacity to switch PNAG production off could benefit the bacteria *in vivo*. It could also benefit the bacteria in conditions that favor the planktonic mode of growth.

The 5 bp deletion in the MN8m *ica* promoter leads to constitutive *icaADBC* transcription and the accumulation of at least 300-fold more transcript than the clinical isolate parent strain MN8. Such high-level transcript production and protein synthesis would seem to be metabolically costly even in the absence of PNAG production. We therefore found it somewhat surprising that the most common mutation (7 out of 12 variants) occurred within the last gene in the operon (*icaC*) and that transcript and Ica proteins were still being produced at MN8m levels. Furthermore, the insertion sequence IS256 has been shown to turn PNAG synthesis off through insertional inactivation of *icaC* (Kiem et al., 2004) suggesting again that mutation of IcaC is the preferred “off switch” for PNAG production. We tested our hypothesis that there might be some advantage to continuing synthesis of IcaA, IcaD, and IcaB even though PNAG is not produced in the absence of IcaC. Our results indicate that under nutrient-limiting conditions, possession of functional *icaADB* genes was advantageous for survival. It is possible that in the absence of functional IcaC, the remaining proteins are still capable of producing PNAG precursor oligomers within the cell. Therefore, perhaps these N-acetylglucosamine oligomers can function as a reserve store of UDP-N-acetyl-

glucosamine under nutrient-limiting conditions and can be degraded to provide N-acetylglucosamine for other cellular process such as cell wall synthesis. Further work is needed to more clearly elucidate the roles of the IcaA, IcaD, and IcaB proteins alternative to their function in PNAG synthesis.

We found that 7 out of 12 of the non-mucoid variants isolated in this study exhibited an insertion or deletion of 4 bp within a region of simple "ttta" repeats. In JB12, a "ttta" repeat insertion extends the repeats in this region from three units to four. This is likely to be the result of slipped-strand mispairing during DNA replication. The mutation shifts the reading frame, leading to a premature stop codon and truncates the protein at 303 amino acids, 47 amino acids shorter than the full-length protein. Structural prediction indicates that the mutation disrupts a transmembrane domain of IcaC, suggesting that if the truncated protein is present in the bacteria, its location may be altered. We have preliminary evidence that supports the idea that this phase variation does have some *in vivo* relevance, since five clinical isolates have thus far been identified as possessing variations in the number of "ttta" repeats in this region. However, *in vitro* examination of the phenotypic effect of these variable numbers of repeats needs to be performed.

CHAPTER 5

Evidence of polarity/translational coupling between *icaB* and *icaC* of *Staphylococcus aureus*

Introduction

A polar mutation affects the expression of distal genes, and is a frequent occurrence in prokaryotes. Commonly, a nonsense, frameshift, or insertion mutation near the promoter proximal region of an upstream gene in a co-transcribed operon significantly reduces the transcription or translation of downstream genes. One type of bacterial polarity affecting translation of an operon is called translational coupling. Translational coupling occurs when complete translation of a gene is necessary for efficient translation of a downstream gene, and was first identified in the *E. coli* tryptophan operon (Aksoy *et al.*, 1984). Coupled genes are commonly found to have overlapping translational start/stop sites, and the genes products are usually present in equimolar complexes. Translational coupling is therefore proposed as a molecular mechanism for maintaining stoichiometric balance between proteins in a synthetic pathway (Aksoy et al., 1984, Oppenheim & Yanofsky, 1980). There are currently three supported models of translational coupling. The first type occurs when base-pair structure within the mRNA masks the initiation site of the downstream gene, and a translating ribosome from the upstream gene is required to disrupt the secondary

structure when in proximity, exposing the start site and enabling translation exclusively by free ribosomes (Berkhout & van Duin, 1985). The second model relies on the same presence of secondary structure occluding the translational start site of the downstream gene, but the presence of the upstream translating ribosomes enables translation by either free ribosomes or continuation of the bound ribosomes (Berkhout *et al.*, 1987, Das & Yanofsky, 1989). The third model of translational coupling occurs when there is poor binding of free ribosomes to the Shine-Delgarno sequence, or ribosomal binding site, of the downstream gene and only bound ribosomes from the upstream gene can efficiently reinitiate translation upon pausing at the overlap region (Govantes *et al.*, 1998, Ivey-Hoyle & Steege, 1992).

In the present study we continued our work characterizing the different molecular mechanisms responsible for the frequent non-mucoid variants that were previously observed to accumulate in mucoid *Staphylococcus aureus* strain MN8m cultures. While the majority of the mutations identified thus far were located in the *icaC* gene and characterized by complete loss of PNAG production, another non-mucoid variant was found to have a nonsense mutation in *icaB* producing the same phenotype. Given that previous efforts to delete the *icaB* gene in *S. aureus* did not result in a similar phenotype, we reasoned that the method of deletion by allelic exchange may have masked an underlying, previously unknown relationship between *icaB* and the downstream gene *icaC*. We therefore hypothesized that a nonsense mutation early in *icaB* would have a polar effect on expression of *icaC*, most likely through translational coupling of the genes since the stop site of *icaB* overlaps with the start site of *icaC*. Our investigation into this phenomenon thus far has supported polarity between the genes,

and begun to elucidate the potential for translational coupling although the exact nature has yet to be fully defined.

Results

Isolation of biofilm-deficient, MN8m non-mucoid variant JB17

As previously outline in Chapter 5, non-mucoid variants have been found to accumulate in pure cultures of the mucoid *S. aureus* strain MN8m. When these cultures were plated on Congo red agar (CRA), both mucoid colonies, which appear dry with irregular edges, and non-mucoid colonies, which are slick, circular, and occasionally surrounded by a transparent red perimeter, were observed (Fig. 14). Of the non-mucoid MN8m variants isolated, one named JB17 was also selected for further characterization. We compared the biofilm-forming ability of this non-mucoid variant to MN8 (the strain from which MN8m derived), which produces a low level of PNAG (considered wild-type), and to the PNAG-negative strain MN8*Δica* (Fig. 26). The JB17 strain displayed a significant decrease in biofilm formation, most closely resembling the PNAG-negative strain MN8*Δica*.

Analysis of non-mucoid variant JB17 to determine PNAG expression

The finding that JB17 biofilms resembled those of the PNAG-negative strain MN8*Δica* suggested that PNAG production was severely abrogated or absent in JB17. To test this, we performed slot-blot analysis using PNAG-specific rabbit polyclonal antiserum. As depicted in Figure 27, no PNAG was detected on the cell surface or in the spent media of JB17 cultures. Therefore, the molecular mechanism leading to the

Figure 26. Biofilm formation by the non-mucoid variant, JB17. Biofilm formation was assessed by visualization of biofilms formed on microtiter plate wells by safranin staining and quantitative data was obtained by resuspending the safranin in acetic acid. Bars represent the mean $OD_{562\ nm}$ of n = 6, and error bars indicate the standard deviations. Statistical comparison (unpaired t test) of MN8m versus JB17 gave a P value of <0.001.

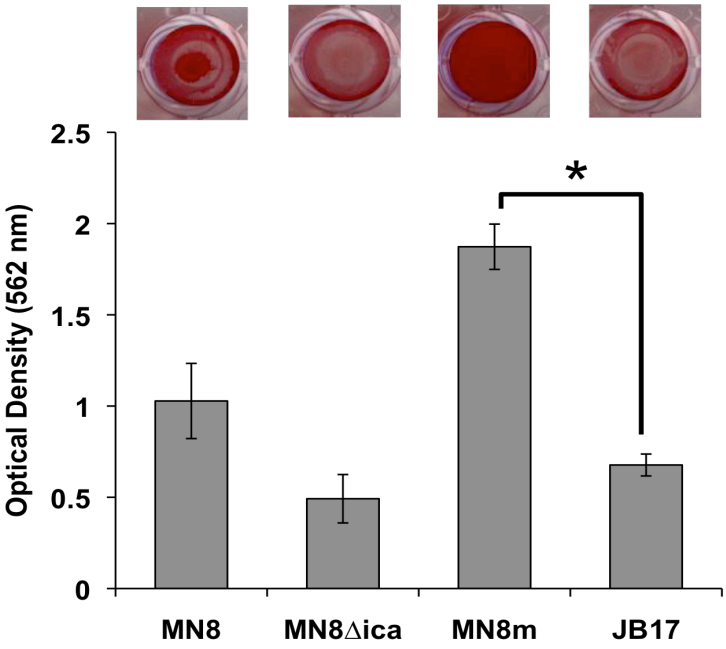

Figure 27. PNAG production by the non-mucoid variant, JB17. PNAG slot blot analysis of *S. aureus* strains producing different amounts of PNAG; probed with PNAG-specific polyclonal antiserum. Samples for both MN8m cell surface and spent media were diluted 1:10 prior to immobilization on membrane.

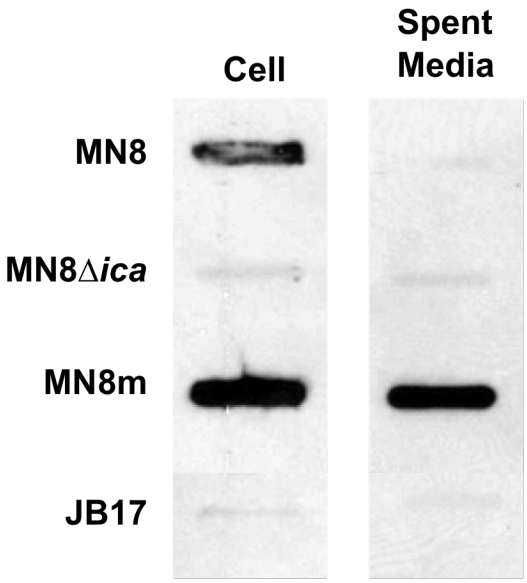

non-mucoid phenotype appeared to be mediating the variation through the loss of detectable levels of PNAG, similar to the initial observations of the previously characterized non-mucoid variant JB12, although not necessarily caused by the same mechanism.

icaADBC transcript level of JB17

A 5 bp deletion in the *icaADBC* promoter region of MN8m is responsible for constitutive *icaADBC* transcription and the constitutive hyper-production of PNAG that characterizes strain MN8m (Jefferson et al., 2003). We sequenced this region of DNA in strain JB17 and found that the 5 bp deletion was identical to MN8m. The *icaADBC* genes are co-transcribed, so to determine levels of the full-length transcript, we quantified levels of the 3'-most transcript, *icaC*, by realtime RT-PCR. As shown in Figure 28, *icaADBC* transcript levels were more than 300-fold greater in MN8m than in the non-mucoid parent strain MN8 and the level remained elevated in the non-mucoid variant JB17. These results indicate that the loss of PNAG production was not due to a decrease in the level of *icaADBC* transcript, but rather that it was mediated by a mechanism affecting PNAG synthesis.

Identification of a nonsense mutation in *icaB* of strain JB17

Since the 5 bp promoter deletion remained and there was no detectable difference in i*caADBC* transcript levels, DNA sequencing of the entire operon was performed. A deletion of two base pairs near the beginning of *icaB* was found (Fig. 29),

Figure 28. Levels of *ica* transcript in the non-mucoid variant, JB17. Real-time RT-PCR analysis of *icaC* mRNA transcript was performed. Bars represent the mean fold difference in transcript amount relative to strain MN8 with n = 3, and error bars indicate the standard deviations. Statistical comparison (unpaired t test) of MN8m and JB17 versus MN8 gave a P value of <0.001.

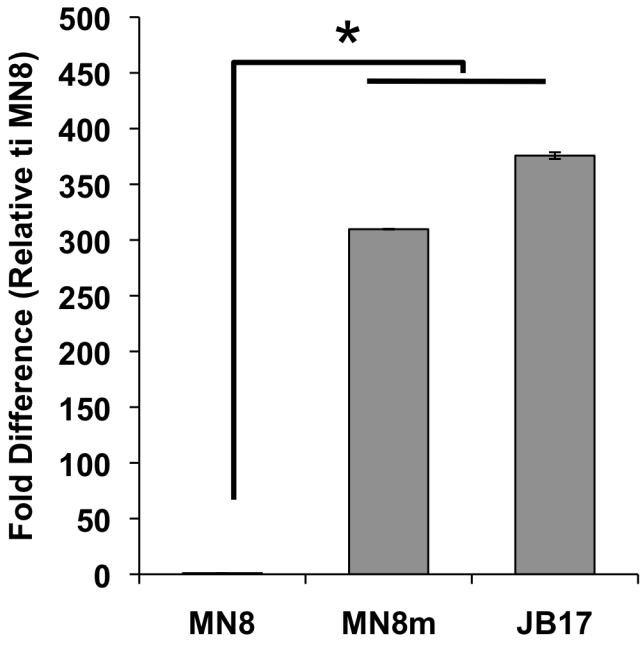

causing a shift of translational reading frame and truncation of the protein; reducing IcaB from 290 amino acids to 62.

However, previous work in our lab has shown that, while deletion of *icaB* prevents surface association by preventing deacetylation of PNAG, it does not cause a loss of PNAG production (Cerca *et al.*, 2007). Instead, the PNAG is released into the spent medium. Yet the PNAG slot blot of strain JB17 (Fig. 27), which was now known to be an *icaB* mutant, did not show any PNAG present in the spent media. Therefore, we hypothesized that the nonsense mutation in *icaB* might have a polar effect on the expression of the downstream gene *icaC*, leading to the observed loss of PNAG production. In our efforts to confirm that the nonsense mutation was responsible for loss of the mucoid phenotype, we complemented the *icaB* gene *in trans* using the plasmid pCL15. Given our hypothesis, we also complemented JB17 *in trans* with either *icaBC*, *icaC* with the native Shine-Delgarno sequence intact, or *icaC* with the Shine-Delgarno sequence modified to an ideal consensus sequence. Only expression of the intact *icaBC* gene in strain JB17 from the IPTG-inducible plasmid pCL15 restored the mucoid biofilm formation (Fig. 30) and PNAG synthesis (Fig. 31). Introduction of the empty vector into the variant, or the other genes had no effect.

Discussion

We have isolated a non-mucoid variant from the mucoid strain MN8m that is characterized by a loss of PNAG expression and biofilm formation. The mutation responsible for the phenotype variation was shown to have no effect on *icaADBC*

Figure 29. Schematic representation of the *ica* locus showing the position of the nonsense mutation identified in *icaB* of the non-mucoid variant JB17. The sequence highlighted in blue indicates *icaB*, the sequence highlighted in red indicates *icaC*, and the overlapping region of these two genes is highlighted in purple.

Figure 30. Effect of complementation in trans of JB17 with *icaB*, *icaBC*, or *icaC* with native/modified ribosomal binding site on biofilm formation. Biofilms formed in TSBG or TSBG+Cm+1mM IPTG on microtiter plate wells were stained with safranin and the safranin was quantified by resuspending in acetic acid and measuring $OD_{562\ nm}$. Bars represent the mean of 6 replicates, and error bars indicate the standard deviations. Statistical comparison (unpaired t test) of JB17+pCL15 (empty vector) versus JB17+pCL15-*icaBC* gave a P value of <0.001.

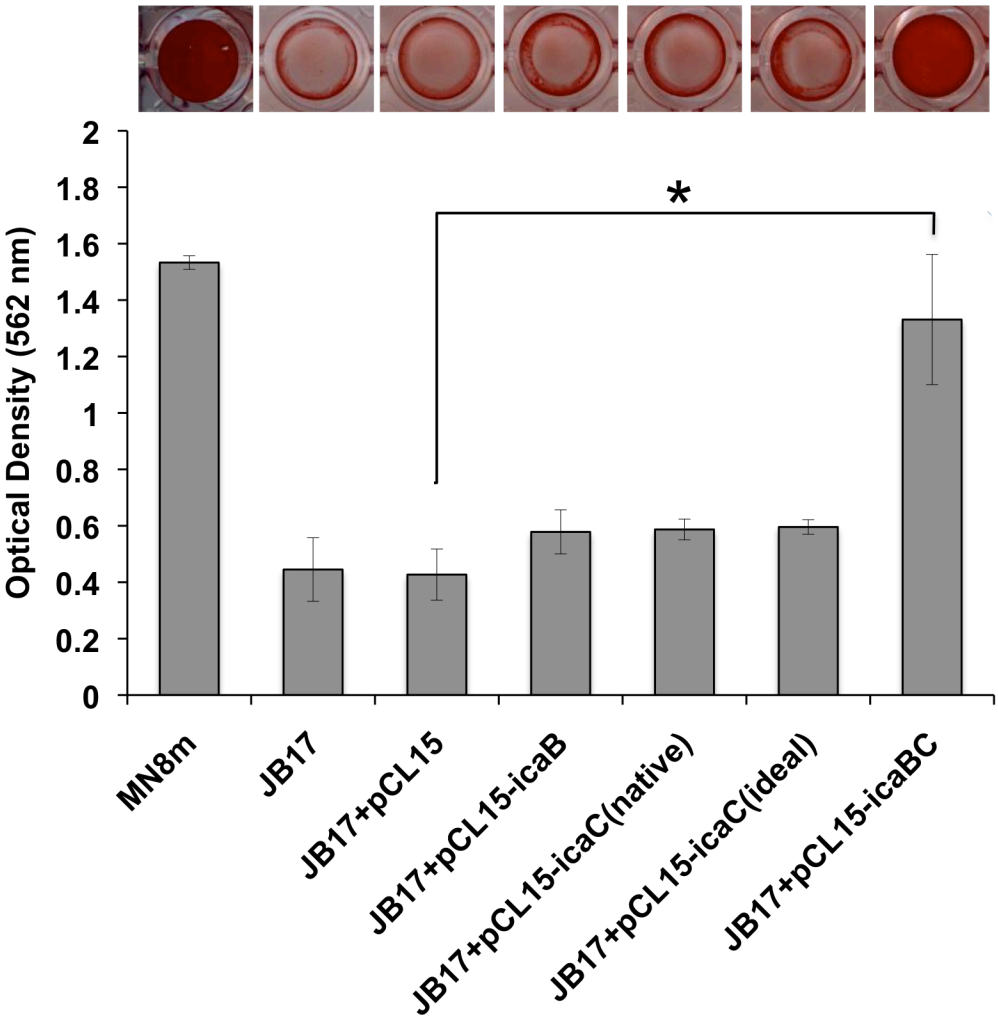

Figure 31. Effect of complementation *in trans* of JB17 with *icaB*, *icaBC*, or *icaC* with native/modified ribosomal binding site on PNAG production. PNAG slot blot of cell surface fractions cultured in TSBG or TSBG+Cm+1mM IPTG probed with polyclonal anti-PNAG antiserum (MN8m and JB17+pCL15-i*caBC* samples were diluted 1:10 prior to immobilization on membrane whereas JB17 and the other JB17+pCL15 strains were not diluted).

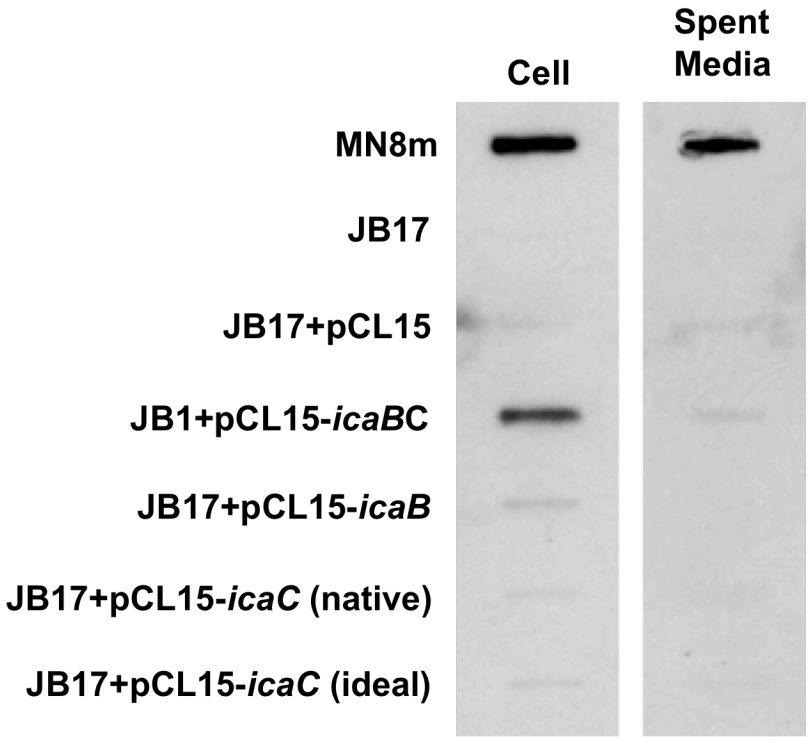

transcript levels despite the absence of PNAG expression, and was identified as a 2-bp deletion in *icaB* leading to a shift in translational reading frame (a nonsense mutation). Since IcaB is responsible for partial deacetylation of PNAG polymers, allowing them to remain surface associated, it is reasonable to expect an IcaB-negative mutant would produce full-length highly-acetylated PNAG that is released into the supernatant. This theory is supported by our previous work showing exactly this occurrence in *S. aureus* in which the *icaB* gene was deleted through in-frame removal of approximately 80% (Cerca et al., 2007). However, our work in this current study showed that the *icaB* nonsense mutant strain JB17 produced no detectable PNAG, either on the cell surface or in the culture supernatant. Additionally, complementation *in trans* of intact IcaB did not restore any detectable production or surface expression of PNAG. These results indicate that the use of the common techniques of creating a null mutant through allelic replacement or deleting a majority of the gene but leaving the remaining portion in frame, may have masked a previously unknown role of the *icaB* gene in the expression of the PNAG synthesis pathway.

Polarity between multiple genes in a co-transcribed operon is very common in prokaryotes, and is almost certainly relevant to these observations. IcaC is thought to be responsible for assembly of full-length PNAG polymers within the cell and translocating them to the cell surface, and is therefore considered an indispensable part of the PNAG synthesis pathway. We therefore hypothesized that a nonsense mutation early in *icaB* would have a polar effect on expression of *icaC*, leading to the loss of function of both gene products. Our observations that *icaC* transcript levels are not diminished by the mutation indicate that the polar effect does not alter transcription of

the downstream gene, meaning that the effect is most likely through translational coupling of the genes.

A specific nucleotide mutation is not in itself polar, instead the large region left untranslated between the two genes is (Zipser, 1969). Mutational studies have previously supported the importance of translation stopping at its normal site in close proximity to the start of the distal gene. Altering translation termination closer to the promoter increases the untranslated region and increases the polar effect, further reducing translation of the downstream gene. This has been shown to be due to one of the three models of translational coupling, all of which are dependent on ribosomes translating the upstream gene coming into close physical proximity to the initiation site of the downstream gene to either: relieve secondary structure occluding the start site, or to 'slide' after pausing and reinitiate translation themselves because free ribosomes are unable to recognize it. Our discovery that *icaC* complementation *in trans* did not restore PNAG production or secretion into the supernatant, led us to investigate the possibility that this last type of translational coupling was responsible for the JB17 phenotype. We tested this theory by expressing a modified version of the *icaC* gene *in trans*. It was modified by the replacement of the native ribosomal binding site with an optimized Shine-Delgarno sequence, which we hypothesized would restore PNAG production into the supernatant if poor binding of free ribosomes was responsible for the loss of translation. However, we were able to conclude that optimizing the ribosomal binding site of *icaC* so that it can be 'seen' by free ribosomes is not sufficient to restore PNAG production. Therefore, it is still possible that mRNA secondary structure at the translation initiation site of *icaC* is preventing translation because ribosomes translating

icaB prematurely disassociate too far upstream, an effect which might still be observed if the same base-pair structure is present in the mRNA originating from the plasmid encoded copy of *icaC* during complementation. To this point, our investigation into this phenomenon has thus supported a polar relationship between the genes *icaB* and *icaC*, and begun to elucidate the potential for translational coupling although the exact nature has yet to be fully defined.

Our work has also addressed a common observation in other examples of polar mutations: the existence of two species of mRNA, both full-length versions and shortened transcripts that terminate near the mutation site (Zipser, 1969). Real-time RT-PCR analysis of *icaADBC* transcription utilized *icaC* primers that are seated well downstream of the nonsense mutation in *icaB,* and showed no significant difference in *icaC* transcript level indicating that full-length mRNA is the dominant species in this particular example of polarity. A Northern blot could be used to more conclusively determine whether both potential species of mRNA are present and at what level.

CHAPTER 6

Conclusions and Future Perspectives

Although the role of PNAG in *S. aureus* biofilms is perhaps the most studied of the potential adhesive molecules of the extracellular polymeric matrix, our knowledge is incomplete. The goal of this project was to utilize a strain that over-produces PNAG to better elucidate details of the expression and regulation of the *icaADBC* operon responsible for PNAG synthesis. We sought first to better understand promoter-regulator interactions and promoter characteristics that influence transcriptional activation, and then to explore new evidence that PNAG expression can be modulated by phase variation within a biofilm population to reduce its contribution.

The initial research focus of this project was to characterize the molecular mechanism underlying the 5 bp deletion in the *S. aureus* MN8m *ica* promoter region that is responsible for the conversion to mucoid PNAG hyper-production. We were able to conclude that the deletion has no effect on the intrinsic curvature of what we determined to be a linear region of DNA in the *ica* promoter. The deletion also has no apparent effect on the binding affinity of the positive regulator SarA, despite the fact that it disrupts a putative binding site. In the process of determining this lack of binding perturbation, it was noted that there are multiple potential binding SarA binding sites in the region selected and that binding of multiple proteins does occur *in vitro*. Therefore

further work should be devoted to determining if any specific sequence or site is a preferred binding sites within this region, which would help to provide insight into the current debate over whether SarA targets a nucleotide consensus sequence or a specific type of DNA structural topology for binding. Beyond these initial investigations into the characteristics of the MN8m promoter, we have concluded that the promoter deletion renders SarA no longer necessary for *ica* transcriptional activation. In this strain background, SarA does not act as a positive regulator of the *icaADBC* operon as it known to be; instead SarA functions as a negative regulator to inhibit transcriptional activation.

In the process of working with strain MN8m we were given the opportunity to explore a phenomenon casually observed by handling liquid MN8m cultures: the frequent occurrence of what appeared to be a non-mucoid sub-population. This has led us to truly novel discoveries about regulation and expression of PNAG. Most notably, we have identified a novel mechanism for switching off PNAG production through the slipped-strand mispairing-mediated inactivation of IcaC. *In vitro*, elevated production of PNAG carried a fitness cost and consequently, PNAG-negative phase variants quickly increased in number relative to PNAG over-expressers. IcaC appears to be the chosen target for phase variation in PNAG production and loss of this protein appears to confer a survival advantage under nutrient-poor conditions relative to the loss of the entire operon, suggesting that the other proteins encoded within the *ica* locus could have some other function. The next step from this point would be to confirm that these remaining genes are in fact functional as we suppose by determining if the first two steps of the PNAG synthesis involving *icaAD* are still occurring. This could be

accomplished by detecting PNAG-precursors within the bacterial cell, and could also provide information about the function of the transmembrane domain lost in the *icaC* variation if short oligomers of PNAG versus full length polymers are found; i.e. does the mutation affect assembly or translocation function of IcaC? Evidence of this mechanism of phase variation in clinical isolates has supported the *in vivo* relevance of our observations, although future work needs to be devoted to confirming the predicted phenotype change resulting from variable repeats. Further pursuit of these variant clinical isolates may have greater implications in virulence and disease manifestation.

While characterizing the non-mucoid variants isolated from MN8m that possess *icaC* mutations, we identified a mutant that was phenotypically identical but had a nonsense mutation further upstream in *icaB*. This mutant did not secrete full length PNAG into the surrounding milieu, as previous *icaB* mutational studies suggested it should. We concluded that our previous method of generating a null mutant had prevented the observation of a polar relationship between *icaB* and its downstream gene *icaC*, a relationship that was supported by restoration of PNAG expression through complementation *in trans* with *icaBC*. There are different types of polar mutation effects, one of which is translational coupling, which we believe is occurring in this operon. The translation termination location is critical in instances of translational coupling, and allelic exchange with an antibiotic cassette would have prevented this polar effect when the ribosome translating the cassette read through it and paused near the *icaC* initiation site, allowing it to then be translated. Our work modifying the Shine-Delgarno sequence indicates that further work is needed to identify the exact mechanism of translational coupling between these two genes, which could be

accomplished by removing the untranslated distance in-frame from between the *icaB* nonsense mutation and *icaC* and by exploring the possibility of mRNA secondary structure at the beginning of *icaC*.

Given the clinical relevance of *Staphylococcus aureus* as an opportunistic pathogen responsible for a large range of infections that affect numerous sites of the human body, research into its expression and regulation of virulence factors could have significant impact of our understanding of their role in disease and potential treatment strategies. Poly-N-acetylglucosamine is a major component of the extracellular polymeric matrix of *S. aureus* biofilms, and its increased expression is sometimes a crucial step in the disease progression of biofilm-associated infections. PNAG is also present on the cell surface even when cells are not part of a biofilm and plays an important role in innate immune evasion, contributing to avoidance of opsonophagocytosis and resistance to antimicrobial peptides. Therefore, having a more complete basic scientific understanding of *icaADBC* expression and regulation could potentially be very useful. The work in this study has identified multiple new levels of *ica* expression regulation, including at the level of transcription through the activity of SarA, of translation through polarity between *icaB* and *icaC*, and modulating PNAG expression by direct nucleotide mutation resulting in phase variation. These observations are significant because cutting-edge therapeutic strategies are currently attempting to target virulence factors rather than viability. Anti-virulence therapies are ideal because they are less likely to result in the propagation of mutations leading to resistance since they exert less selective pressure upon the bacterial population. Therefore, the contributions of this study to our understanding of the regulation of one of

S. aureus' key virulence factors may help to make future anti-virulence strategies more effective.

Literature Cited

Literature Cited

Aksoy, S., C. L. Squires & C. Squires, (1984) Translational coupling of the *trpB* and *trpA* genes in the *Escherichia coli* tryptophan operon. *J Bacteriol* **157**: 363-367.

Berkhout, B., B. F. Schmidt, A. van Strien, J. van Boom, J. van Westrenen & J. van Duin, (1987) Lysis gene of bacteriophage MS2 is activated by translation termination at the overlapping coat gene. *J Mol Biol* **195**: 517-524.

Berkhout, B. & J. van Duin, (1985) Mechanism of translational coupling between coat protein and replicase genes of RNA bacteriophage MS2. *Nucleic Acids Res* **13**: 6955-6967.

Brown, M. R., D. G. Allison & P. Gilbert, (1988) Resistance of bacterial biofilms to antibiotics: a growth-rate related effect? *J Antimicrob Chemother* **22**: 777-780.

Brukner, I., R. Sanchez, D. Suck & S. Pongor, (1995) Sequence-dependent bending propensity of DNA as revealed by DNase I: parameters for trinucleotides. *EMBO J* **14**: 1812-1818.

Cerca, N., K. K. Jefferson, T. Maira-Litran, D. B. Pier, C. Kelly-Quintos, D. A. Goldmann, J. Azeredo & G. B. Pier, (2007) Molecular basis for preferential protective efficacy of antibodies directed to the poorly acetylated form of staphylococcal poly-N-acetyl-beta-(1-6)-glucosamine. *Infect Immun* **75**: 3406-3413.

Cheung, A. L. & A. C. Manna, (2005) Role of the distal *sarA* promoters in SarA expression in *Staphylococcus aureus*. *Infect Immun* **73**: 4391-4394.

Christensen, G. D., W. A. Simpson, J. J. Younger, L. M. Baddour, F. F. Barrett, D. M. Melton & E. H. Beachey, (1985) Adherence of coagulase-negative staphylococci to plastic tissue culture plates: a quantitative model for the adherence of staphylococci to medical devices. *J Clin Microbiol* **22**: 996-1006.

Costerton, J. W., Z. Lewandowski, D. E. Caldwell, D. R. Korber & H. M. Lappin-Scott, (1995) Microbial biofilms. *Annu Rev Microbiol* **49**: 711-745.

Cramton, S. E., C. Gerke, N. F. Schnell, W. W. Nichols & F. Gotz, (1999) The intercellular adhesion (ica) locus is present in *Staphylococcus aureus* and is required for biofilm formation. *Infect Immun* **67**: 5427-5433.

Cramton, S. E., M. Ulrich, F. Gotz & G. Doring, (2001) Anaerobic conditions induce expression of polysaccharide intercellular adhesin in *Staphylococcus aureus* and *Staphylococcus epidermidis*. *Infect Immun* **69**: 4079-4085.

Cucarella, C., C. Solano, J. Valle, B. Amorena, I. Lasa & J. R. Penades, (2001) Bap, a *Staphylococcus aureus* surface protein involved in biofilm formation. *J Bacteriol* **183**: 2888-2896.

Das, A. & C. Yanofsky, (1989) Restoration of a translational stop-start overlap reinstates translational coupling in a mutant *trpB'-trpA* gene pair of the *Escherichia coli* tryptophan operon. *Nucleic Acids Res* **17**: 9333-9340.

Davies, D. G., M. R. Parsek, J. P. Pearson, B. H. Iglewski, J. W. Costerton & E. P. Greenberg, (1998) The involvement of cell-to-cell signals in the development of a bacterial biofilm. *Science* **280**: 295-298.

DeLeo, F. R. & H. F. Chambers, (2009) Reemergence of antibiotic-resistant *Staphylococcus aureus* in the genomics era. *J Clin Invest* **119**: 2464-2474.

Diekema, D. J., M. A. Pfaller, F. J. Schmitz, J. Smayevsky, J. Bell, R. N. Jones & M. Beach, (2001) Survey of infections due to *Staphylococcus* species: frequency of occurrence and antimicrobial susceptibility of isolates collected in the United States, Canada, Latin America, Europe, and the Western Pacific region for the SENTRY Antimicrobial Surveillance Program, 1997-1999. *Clin Infect Dis* **32 Suppl 2**: S114-132.

Foster, T. J., (2005) Immune evasion by staphylococci. *Nat Rev Microbiol* **3**: 948-958.

Fujimoto, D. F., E. W. Brunskill & K. W. Bayles, (2000) Analysis of genetic elements controlling *Staphylococcus aureus lrgAB* expression: potential role of DNA topology in SarA regulation. *J Bacteriol* **182**: 4822-4828.

Fujimoto, D. F., R. H. Higginbotham, K. M. Sterba, S. J. Maleki, A. M. Segall, M. S. Smeltzer & B. K. Hurlburt, (2009) *Staphylococcus aureus* SarA is a regulatory protein responsive to redox and pH that can support bacteriophage lambda integrase-mediated excision/recombination. *Mol Microbiol* **74**: 1445-1458.

Gabrielian, A. & S. Pongor, (1996) Correlation of intrinsic DNA curvature with DNA property periodicity. *FEBS Lett* **393**: 65-68.

Gerke, C., A. Kraft, R. Sussmuth, O. Schweitzer & F. Gotz, (1998) Characterization of the N-acetylglucosaminyltransferase activity involved in the biosynthesis of the *Staphylococcus epidermidis* polysaccharide intercellular adhesin. *J Biol Chem* **273**: 18586-18593.

Govantes, F., E. Andujar & E. Santero, (1998) Mechanism of translational coupling in the *nifLA* operon of *Klebsiella pneumoniae*. *EMBO J* **17**: 2368-2377.

Gross, M., S. E. Cramton, F. Gotz & A. Peschel, (2001) Key role of teichoic acid net charge in *Staphylococcus aureus* colonization of artificial surfaces. *Infect Immun* **69**: 3423-3426.

Howden, B. P., J. K. Davies, P. D. Johnson, T. P. Stinear & M. L. Grayson, (2010) Reduced vancomycin susceptibility in *Staphylococcus aureus*, including vancomycin-intermediate and heterogeneous vancomycin-intermediate strains: resistance mechanisms, laboratory detection, and clinical implications. *Clin Microbiol Rev* **23**: 99-139.

Hoyle, B. D. & J. W. Costerton, (1991) Bacterial resistance to antibiotics: the role of biofilms. *Prog Drug Res* **37**: 91-105.

Ivey-Hoyle, M. & D. A. Steege, (1992) Mutational analysis of an inherently defective translation initiation site. *J Mol Biol* **224**: 1039-1054.

Izano, E. A., M. A. Amarante, W. B. Kher & J. B. Kaplan, (2008) Differential roles of poly-N-acetylglucosamine surface polysaccharide and extracellular DNA in *Staphylococcus aureus* and *Staphylococcus epidermidis* biofilms. *Appl Environ Microbiol* **74**: 470-476.

Jefferson, K. K., S. E. Cramton, F. Gotz & G. B. Pier, (2003) Identification of a 5-nucleotide sequence that controls expression of the *ica* locus in *Staphylococcus*

aureus and characterization of the DNA-binding properties of IcaR. *Mol Microbiol* **48**: 889-899.

Keren, I., N. Kaldalu, A. Spoering, Y. Wang & K. Lewis, (2004) Persister cells and tolerance to antimicrobials. *FEMS Microbiol Lett* **230**: 13-18.

Kiem, S., W. S. Oh, K. R. Peck, N. Y. Lee, J. Y. Lee, J. H. Song, E. S. Hwang, E. C. Kim, C. Y. Cha & K. W. Choe, (2004) Phase variation of biofilm formation in *Staphylococcus aureus* by IS 256 insertion and its impact on the capacity adhering to polyurethane surface. *J Korean Med Sci* **19**: 779-782.

Kim, J., C. Zwieb, C. Wu & S. Adhya, (1989) Bending of DNA by gene-regulatory proteins: construction and use of a DNA bending vector. *Gene* **85**: 15-23.

Kreiswirth, B. N., S. Lofdahl, M. J. Betley, M. O'Reilly, P. M. Schlievert, M. S. Bergdoll & R. P. Novick, (1983) The toxic shock syndrome exotoxin structural gene is not detectably transmitted by a prophage. *Nature* **305**: 709-712.

Levinson, G. & G. A. Gutman, (1987) Slipped-strand mispairing: a major mechanism for DNA sequence evolution. *Mol Biol Evol* **4**: 203-221.

Liu, Y., A. C. Manna, C. H. Pan, I. A. Kriksunov, D. J. Thiel, A. L. Cheung & G. Zhang, (2006) Structural and function analyses of the global regulatory protein SarA from *Staphylococcus aureus*. *Proc Natl Acad Sci U S A* **103**: 2392-2397.

Mack, D., W. Fischer, A. Krokotsch, K. Leopold, R. Hartmann, H. Egge & R. Laufs, (1996) The intercellular adhesin involved in biofilm accumulation of *Staphylococcus epidermidis* is a linear beta-1,6-linked glucosaminoglycan: purification and structural analysis. *J Bacteriol* **178**: 175-183.

Maira-Litran, T., A. Kropec, C. Abeygunawardana, J. Joyce, G. Mark, 3rd, D. A. Goldmann & G. B. Pier, (2002) Immunochemical properties of the staphylococcal poly-N-acetylglucosamine surface polysaccharide. *Infect Immun* **70**: 4433-4440.

Maira-Litran, T., A. Kropec, D. A. Goldmann & G. B. Pier, (2005) Comparative opsonic and protective activities of *Staphylococcus aureus* conjugate vaccines containing native or deacetylated Staphylococcal Poly-N-acetyl-beta-(1-6)-glucosamine. *Infect Immun* **73**: 6752-6762.

Majerczyk, C. D., M. R. Sadykov, T. T. Luong, C. Lee, G. A. Somerville & A. L. Sonenshein, (2008) *Staphylococcus aureus* CodY negatively regulates virulence gene expression. *J Bacteriol* **190**: 2257-2265.

McKenney, D., J. Hubner, E. Muller, Y. Wang, D. A. Goldmann & G. B. Pier, (1998) The *ica* locus of *Staphylococcus epidermidis* encodes production of the capsular polysaccharide/adhesin. *Infect Immun* **66**: 4711-4720.

Nannini, E., B. E. Murray & C. A. Arias, (2010) Resistance or decreased susceptibility to glycopeptides, daptomycin, and linezolid in methicillin-resistant *Staphylococcus aureus*. *Curr Opin Pharmacol*.

Oppenheim, D. S. & C. Yanofsky, (1980) Translational coupling during expression of the tryptophan operon of *Escherichia coli*. *Genetics* **95**: 785-795.

Perez-Martin, J. & V. de Lorenzo, (1997) Clues and consequences of DNA bending in transcription. *Annu Rev Microbiol* **51**: 593-628.

Sander, P., B. Springer, T. Prammananan, A. Sturmfels, M. Kappler, M. Pletschette & E. C. Bottger, (2002) Fitness cost of chromosomal drug resistance-conferring mutations. *Antimicrob Agents Chemother* **46**: 1204-1211.

Schlievert, P. M. & D. A. Blomster, (1983) Production of staphylococcal pyrogenic exotoxin type C: influence of physical and chemical factors. *J Infect Dis* **147**: 236-242.

Schumacher, M. A., B. K. Hurlburt & R. G. Brennan, (2001) Crystal structures of SarA, a pleiotropic regulator of virulence genes in *S. aureus*. *Nature* **409**: 215-219.

Tormo, M. A., M. Marti, J. Valle, A. C. Manna, A. L. Cheung, I. Lasa & J. R. Penades, (2005) SarA is an essential positive regulator of *Staphylococcus epidermidis* biofilm development. *J Bacteriol* **187**: 2348-2356.

Vlahovicek, K., L. Kajan & S. Pongor, (2003) DNA analysis servers: plot.it, bend.it, model.it and IS. *Nucleic Acids Res* **31**: 3686-3687.

Vuong, C., S. Kocianova, J. M. Voyich, Y. Yao, E. R. Fischer, F. R. DeLeo & M. Otto, (2004a) A crucial role for exopolysaccharide modification in bacterial biofilm formation, immune evasion, and virulence. *J Biol Chem* **279**: 54881-54886.

Vuong, C., J. M. Voyich, E. R. Fischer, K. R. Braughton, A. R. Whitney, F. R. DeLeo & M. Otto, (2004b) Polysaccharide intercellular adhesin (PIA) protects *Staphylococcus epidermidis* against major components of the human innate immune system. *Cell Microbiol* **6**: 269-275.

Walters, M. C., 3rd, F. Roe, A. Bugnicourt, M. J. Franklin & P. S. Stewart, (2003) Contributions of antibiotic penetration, oxygen limitation, and low metabolic activity to tolerance of *Pseudomonas aeruginosa* biofilms to ciprofloxacin and tobramycin. *Antimicrob Agents Chemother* **47**: 317-323.

Zipser, D., (1969) Polar mutations and operon function. *Nature* **221**: 21-25.

Vita

Jamie Lynn Brooks (née Leftwich) was born on February 8, 1983 in Hampton Virginia and is an American citizen. She graduated from Warwick High School, Newport News, Virginia in 2001. She received her Bachelor of Science in Biomedical Science from Lynchburg College, Lynchburg, Virginia in 2006 and subsequently entered the doctoral graduate program at Virginia Commonwealth University's School of Medicine, Richmond, Virginia. She received her Doctorate of Philosophy from the Department of Microbiology and Immunology at VCU in 2012.

Publications:

Cerca, N. K., Brooks, J. L., & K. K. Jefferson, (2008) Regulation of the intercellular adhesin locus regulator (icaR) by SarA, sigmaB, and IcaR in *Staphylococcus aureus. J Bacteriol* **190**: 6530-6533.

Brooks, J. L. & K. K. Jefferson, (2012) Chapter Two – Staphylococcal Biofilms: Quest for the Magic Bullet. In: Advances in Applied Microbiology. M. G. Geoffrey & S. Sima (eds). Academic Press, pp. 63-87.

Manuscripts in preparation and review:

Brooks, J. L. & K. K. Jefferson. Phase variation of poly-N-acetylglucosamine expression by slipped-strand mispairing in *Staphylococcus aureus*.

Abstracts and Presentations:

Brooks, J. L. & K. K. Jefferson. Staphylococcal polysaccharide production: selection against PNAG overproduction. International Conference on Gram Positive Pathogens, Omaha, NE. 2012. (Presentation)

Brooks, J. L. & K. K. Jefferson. Characterization of the effect of poly-N-acetyl-glucosamine on *Staphylococcus aureus* resistance. American Society of Microbiology – Virginia Branch, Lynchburg College, Lynchburg, VA. 2010. (Presentation)

Brooks, J. L. & K. K. Jefferson. Effect of poly-N-acetylglucosamine expression on *Staphylococcus aureus* surface charge. 111th General Meting American Society of Microbiology, New Orleans, LA. 2011. (Poster)

Brooks, J. L. & K. K. Jefferson. Characterization of the effect of poly-N-acetyl-glucosamine (PNAG) on *Staphylococcus aureus* antibiotic resistance. Daniel T. Watts Symposium, VCU, Richmond, VA. 2010. (Poster)

Awards and Honor Societies:

Travel Award, International Conference on Gram Positive Pathogens (2012)